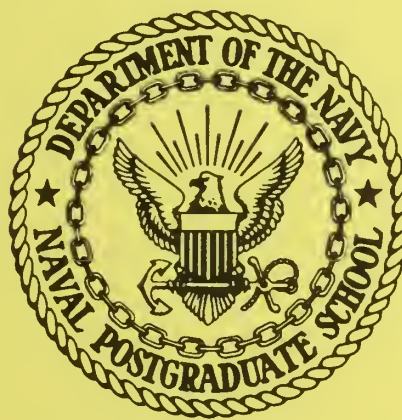


NPS-59Cg74111

NAVAL POSTGRADUATE SCHOOL

Monterey, California



A LIQUID CRYSTAL THERMOGRAPHIC STUDY OF A HEATED CYLINDER IN CROSS FLOW

Thomas E. Cooper

Richard J. Field

John F. Meyer

November 1974

Annual Report for Period January 1974-October 1974

Approved for public release; distribution unlimited

Prepared for:

Chief of Naval Research, Arlington, Virginia 22217, and
Naval Weapons Center, China Lake, California 93555

NAVAL POSTGRADUATE SCHOOL
Monterey, California

Rear Admiral Isham Linder
Superintendent

Jack R. Borsting
Provost

This task was jointly supported by the Foundation Research Program of the Naval Postgraduate School with funds provided by the Chief of Naval Research, Arlington, Virginia and the Naval Weapons Center, China Lake, California.

Reproduction of all or part of this report is authorized.

This report was prepared by:

UNCLASSIFIED

SECURITY CLASSIFICATION OF THIS PAGE (When Data Entered)

| REPORT DOCUMENTATION PAGE | | READ INSTRUCTIONS BEFORE COMPLETING FORM |
|---|-----------------------|---|
| 1. REPORT NUMBER NPS-59Cg74111 | 2. GOVT ACCESSION NO. | 3. RECIPIENT'S CATALOG NUMBER |
| 4. TITLE (and Subtitle) A LIQUID CRYSTAL THERMOGRAPHIC STUDY OF A HEATED CYLINDER IN CROSS FLOW | | 5. TYPE OF REPORT & PERIOD COVERED Annual Report 1 January 1974-31 October 74 |
| 7. AUTHOR(s) Thomas E. Cooper Richard J. Field John F. Meyer | | 6. PERFORMING ORG. REPORT NUMBER |
| 9. PERFORMING ORGANIZATION NAME AND ADDRESS Naval Postgraduate School Monterey, California 93940 | | 10. PROGRAM ELEMENT, PROJECT, TASK AREA & WORK UNIT NUMBERS 61152N;RR000-01-10;WR5-0001 F32-311-005;PO-4-0168 |
| 11. CONTROLLING OFFICE NAME AND ADDRESS Chief of Naval Research, Arlington, Va. 22217 Naval Weapons Ctr, China Lake, California 93555 | | 12. REPORT DATE November 1974 |
| 14. MONITORING AGENCY NAME & ADDRESS(if different from Controlling Office) | | 13. NUMBER OF PAGES 51 |
| | | 15. SECURITY CLASS. (of this report) Unclassified |
| | | 15a. DECLASSIFICATION/DOWNGRADING SCHEDULE |
| 16. DISTRIBUTION STATEMENT (of this Report) Approved for public release; distribution unlimited. | | |
| 17. DISTRIBUTION STATEMENT (of the abstract entered in Block 20, if different from Report) | | |
| 18. SUPPLEMENTARY NOTES | | |
| 19. KEY WORDS (Continue on reverse side if necessary and identify by block number) | | |
| 20. ABSTRACT (Continue on reverse side if necessary and identify by block number) A thermographic technique is presented that allows visual determination of both qualitative and quantitative heat transfer and fluid flow information to be obtained on heated objects placed in forced convection environments. The technique employs cholesteric liquid crystals as the temperature sensing agent. The liquid crystals indicate temperature by exhibiting brilliant changes in color over discrete, reproducible temperature ranges. The technique has been used to quickly and easily obtain information on the variation | | |

UNCLASSIFIED

SECURITY CLASSIFICATION OF THIS PAGE(When Data Entered)

of the Nusselt number on a right circular cylinder placed in a crossflow of air. In addition to yielding precise quantitative heat transfer information, the liquid crystal thermographic technique afforded the opportunity to visually observe the effects of flow separation, the separation bubble region, the turbulent boundary layer, and the turbulent wake on the surface temperature of the heated cylinder. The experimental results obtained using the liquid crystal thermographic technique are in close agreement with results obtained by other investigators who have used standard measuring techniques.

UNCLASSIFIED

SECURITY CLASSIFICATION OF THIS PAGE(When Data Entered)

TABLE OF CONTENTS

| | Page |
|--|------|
| I. Introduction | 1 |
| II. Background | 2 |
| III. Experimental Apparatus | 10 |
| IV. Liquid Crystal Application and Calibration | 16 |
| V. Experimental Procedure | 19 |
| VI. Results | 30 |
| VII. Summary | 41 |
| References | 45 |
| Distribution List | 50 |
| Form DD 1473 | 51 |

LIST OF FIGURES

- Figure 1: Schematic of Nichrome-wrapped cylinder.
- Figure 2: Photograph taken through an electron microscope of the Temsheet-liquid crystal interface.
- Figure 3: Nichrome-wrapped cylinder instrumented with the liquid crystal tapes. Note the presence of large surface irregularities.
- Figure 4: Photograph of the Temsheet cylinder coated with the eight liquid crystal bands. The colors displayed by the liquid crystals appear as the light gray regions in the black and white photo.
- Figure 5: Sketch of a typical temperature distribution, T , that develops on the surface of a uniformly heated cylinder that loses heat in an amount q_w to a fluid stream. The fluid is at a uniform temperature, T_∞ , and is moving with velocity U_∞ . The conditions depicted are for subcritical flow as evidenced by the presence of a laminar separation at an angle θ_s .
- Figure 6: Sketch of a typical temperature distribution, T , that develops on the surface of a uniformly heated cylinder that loses heat in an amount q_w to a fluid stream. The fluid is at a uniform temperature, T_∞ , and is moving with velocity U_∞ . The conditions depicted are for critical flow as evidenced by the presence of a laminar separation at an angle θ_s , a separation bubble region, a point of reattachment of a turbulent boundary layer at an angle θ_r , and a subsequent separation of the turbulent boundary layer at an angle θ_{st} .
- Figure 7: Schematic of a typical liquid crystal display. The conditions depicted are representative of subcritical flow. The shaded regions on each liquid crystal band represent color.

Figure 8: Schematic of a typical liquid crystal display. The conditions depicted are representative of critical flow. The shaded regions on each liquid crystal band represent color.

Figure 9: Experimental heat transfer results obtained using the liquid crystal thermographic technique.

Figure 10: Comparison of the experimental heat transfer results obtained using the liquid crystal thermographic technique with the results of others.

Figure 11: Photograph of the Temsheet cylinder coated only with liquid crystal S-43. The bending of the isotherms near the top and bottom of the test section indicates the influence of end losses on the temperature field.

Figure 12: Photograph of the alternate hot and cold spots that developed along the separation line of the Temsheet cylinder.

I. INTRODUCTION

This report describes a technique that allows visual determination of both qualitative and quantitative heat transfer and fluid flow information on heated objects placed in forced convection environments. Cholesteric liquid crystals, a commercially available material that exhibits brilliant changes in color over discrete, reproducible temperature bands, are used as the temperature sensor in the technique. By appropriate calibration, the colors displayed by the liquid crystal material can be accurately related to the temperature of the material. This allows one to visually observe select isotherms and, further, can be used to infer the location of points of flow separation and boundary layer reattachment. The colors displayed by the liquid crystal material also give a dramatic indication of the influence of turbulence on surface temperature. In a region of turbulent flow, the colors displayed by the liquid crystal material continuously dim and glow in response to the "scrubbing" action caused by random bursts of cool fluid impacting on the heated surface.

The liquid crystal thermographic technique has been used to determine the circumferential variation of the Nusselt number on a uniformly heated right circular cylinder cooled by forced convection in a crossflow of air. The heated cylinder in crossflow represents a classic heat transfer problem that has been studied both experimentally and theoretically by numerous investigators over the last 40 or so years. As such, it served as an ideal problem to study with the liquid crystal technique since both theoretical and experimental results were available for comparison. In the present investigation, Reynolds numbers were varied from approximately 40,000 to 150,000. This allows the study of both subcritical and critical flow regimes.

Data were obtained on a 10 cm diameter right circular cylinder constructed from a 0.1 cm thick carbon impregnated paper that exhibited an electrical resistivity of 2.5 ohm-cm. The outer surface of the cylinder was coated with a thin layer of the liquid crystal material. A known heat flux was established on the surface of the cylinder by employing the Joulean heating effect produced by passing a constant current longitudinally through the resistive paper. The inner hollow space of the cylinder was firmly packed with glass wool to prevent heat losses into this region. The glass wool also reinforced the cylinder and aided in resisting deformation due to the outer flow.

The Nusselt number results obtained in the present investigation compare within the estimated experimental uncertainty (5%) in the forward stagnation region on the cylinder with the theoretical solutions proposed by Schuh [1]*, Seban and Chan [2], and Perkins and Leppert [3]. Beyond approximately 60°, the experimental results rapidly diverge from the theoretical predictions. This trend is consistent with the experimental results of Giedt [4], Seban [5], and Meyer [6] and is most probably explained by the fact that a pressure distribution based on frictionless fluid flow behavior was used to generate the theoretical curve.

II. BACKGROUND

Liquid Crystals

In 1888, an Austrian botanist, Friedrich Reinitzer, observed that certain organic compounds appeared to possess two melting points, an initial melting point that turned the solid phase to a cloudy liquid and a second melting point at which the cloudy liquid turned clear. Further research revealed that an intermediate phase, or "mesophase," did indeed exist between the pure solid phase and pure liquid phase of some organic

*Numbers in brackets designate references at end of report.

compounds. Reinitzer termed this phase a "liquid crystal phase," an appropriate designation when one considers that the liquid crystal phase exhibits the fluidity of a liquid while at the same time maintaining a degree of the anisotropic, ordered structure of a crystalline solid. Since Reinitzer's original work, a great deal of research concerning the structure of liquid crystals has been carried out resulting in the classification of liquid crystals into one of three categories: smectic, nematic, or cholesteric; the particular category being determined by the molecular structure of the liquid crystal. In the present work, no attempt was made to study the details of the molecular structure of liquid crystals. Excellent papers on this aspect of liquid crystal technology have been published by Brown and Shaw [7], Fergason [8], Fergason and Brown [9], Dreher, Meir and Saupe [10], and Castellano and Brown [11]. Of particular interest in the present investigation were the optical properties exhibited by the liquid crystal phase and the change that may be produced in the light transmitting and scattering properties of thin films of liquid crystal materials when certain fields are impressed on these films.

A variety of externally applied fields including electrical, magnetic, shear, pressure and thermal fields have been found to produce a change in the optical properties of liquid crystals. As an example, nematic liquid crystals, when applied in a very thin film and viewed through a dielectric material such as glass, appear opaque when an electrical field is applied but appear transparent in the absence of the electrical field. Smectic liquid crystals behave in a similar fashion. Although a host of applications have been and more than likely will continue to be found for the nematic and smectic type liquid crystals [12-17], of immediate concern in our investigation has been the response of cholesteric liquid crystals to

thermal fields and the use of this response to obtain both qualitative and quantitative heat transfer information.

Cholesteric liquid crystals, as the name implies, are formed from esters of cholesterol. The property of interest, from a heat transfer point of view, of the cholesteric type liquid crystal concerns its response to temperature. Over a known, reproducible range of temperature, the "event temperature range," the cholesteric liquid crystal will progressively exhibit all colors of the visible spectrum as it is heated through the event temperature range. The phenomena is reversible, repeatable and, with proper care, color can be accurately calibrated with temperature.

The basis for the color change exhibited by the cholesteric type liquid crystal is a property known as circular dichroism. An incident beam of unpolarized white light, on striking a film of cholesteric liquid crystals, is split into two components having electric vectors rotated in opposite directions. One component is transmitted through the film while the other component is scattered. The scattered light possesses a peak wavelength that is a function of temperature and viewing angle. At temperatures below the event temperature range, the liquid crystal film selectively scatters only long wavelength electromagnetic radiation (infrared) and therefore appears colorless. As the material is heated, however, disturbances produced in intermolecular forces result in a slight change in the crystalline structure possessed by the liquid crystal material. This in turn results in a shift in the wavelength of scattered electromagnetic radiation. As the liquid crystal film is brought to a temperature corresponding to the beginning of the event temperature range, a wavelength corresponding to the red portion of the electromagnetic spectrum is scattered. As the temperature of the material is raised

through the event temperature range, one progressively observes red, yellow, green, blue and violet. With a further increase in temperature, the material again appears colorless due to the selective reflection of wavelengths in the ultraviolet portion of the electromagnetic spectrum. If the liquid crystal material is allowed to cool back through the event temperature range, the sequence just described will be reversed. Both the width of the event temperature range and its placement on the temperature scale can be controlled by selecting both the appropriate cholesteric esters and the proportions used in a given formulation. At present, liquid crystals are commercially available with event temperatures ranging from a few degrees below zero to several hundred degrees Celsius. Liquid crystals can be obtained with event temperature spans as small as 1°*C* to as large as 50°*C*. For optimum brilliance, the cholesteric liquid crystals should be applied as a thin film (0.003 cm to 0.006 cm) on a black substrate. The black substrate insures that all light transmitted through the liquid crystal film is absorbed and therefore is not reflected to compete with the desired signal.

Pure liquid crystals, although exhibiting brilliant colors, pose several problems from the point of view of laboratory usage. Once applied to a specimen, the pure liquid crystals deteriorate rapidly with age permitting only a few hours of experimentation. They are also susceptible to contamination with marked alteration in performance resulting from exposure to many common atmospheric contaminants as well as to ultraviolet light. Further, the detection of temperature via a change in color is strongly influenced by viewing angle.

Many of the problems associated with the use of pure cholesteric liquid crystals have either been eliminated or greatly reduced through an

encapsulating process developed by the National Cash Register Company. The encapsulated liquid crystals, referred to appropriately enough as Encapsulated Liquid Crystals, are coated with polyvinyl alcohol. This coating results in the formation of small spheroids with typical diameters on the order of 20-50 microns. In addition to extending the life of the liquid crystals to as long as several years by protecting the raw crystals from the damaging effects of ultraviolet light and atmospheric contaminants, the encapsulation procedure also greatly reduces the variation of color due to viewing angle. Further, unlike the pure liquid crystals, the encapsulated liquid crystals are relatively insensitive to the effects of normal and shearing forces. Encapsulated liquid crystals can be obtained in one of two forms, either precoated on a blackened substrate of paper or mylar or in a water based slurry. For our experiments, the encapsulated liquid crystals were obtained in slurry form which allowed manual coating of the specimen surface with an ordinary brush.

Prior Work

Cholesteric liquid crystals have been employed in a number of interesting applications over the past several years. To date, the majority of uses have involved qualitative interpretation of the temperature fields displayed so colorfully by the liquid crystals, that is to say, observing hot and cold regions without regard to precise temperature levels. In the field of non-destructive testing, liquid crystals have been used to check for irregularities on bonded structures [18-20], to observe regions of overheating on electronics equipment [15, 19, 20], to check for flow blockages in heat exchangers [21], as crack detectors on aircraft structure [21], and to check the effectiveness of windshield heaters [15, 21, 23], to name but a few typical applications. In the medical field, cholesteric

liquid crystals have been used to observe surface blood flow patterns in humans and as a diagnostic tool for the detection of breast cancer [23-25]. Cholesteric liquid crystals have also been used to study the characteristics of laser beams and ultrasonic beams [26, 27].

Several investigators have employed liquid crystals as the temperature transducer in engineering heat transfer studies. Raad and Myers [28] used liquid crystals to observe nucleation sites in a study of pool boiling. Ennulat and Fergason [29] employed a liquid crystal film as the display device in a non-contacting thermal imaging system. Maple [30] studied the transient and steady state temperature fields that develop on the exterior of an active sonar transducer by coating the surface of the transducer with liquid crystals. Cooper and Groff [31], Katz and Cooper [32], and Cooper and Petrovic [33] employed liquid crystals coated on thin mylar sheets to observe the temperature fields produced by resistively heated, radio-frequency, and cryosurgical cannulas, respectively.

The use of cholesteric liquid crystals in wind tunnel experiments was first investigated by Klein [34, 35] in 1968. Prior to Klein's study, however, Jones and Hunt [36, 37] employed a coating of temperature sensitive material to obtain quantitative heat transfer information on aerodynamically heated bodies. Kaufman, Leng and Johnson [38] used this technique in a similar investigation of aerodynamically heated bodies. The temperature sensitive coatings used in thermographic technique developed by Jones and Hunt were not of the liquid crystal family, however. They were organic substances that underwent an irreversible phase change, changing from an opaque solid to a clear liquid, at known temperatures. The variation of the local heat transfer coefficient on the surface of an aerodynamically heated object is determined as follows. The surface of the object under

investigation is first coated with the temperature sensitive material. A hypersonic flow is established in the wind tunnel. At time zero the model is quickly introduced into the flow. The temperature sensitive coating initially indicates a phase change on the portion of the object experiencing the greatest aerodynamic heating rate. By taking motion pictures of the model, the location of the phase change line can be determined as a function of time. The local convective coefficient is then determined by matching the experimentally determined lines of constant temperature with an analytical solution to the problem containing the convective coefficient as one of the parameters. The value of the convective coefficient that brings theory and experiment into harmony is deemed the correct result.

Although a very clever concept, the thermographic technique developed by Jones and Hunt suffers from several major drawbacks. The technique is transient requiring that the ratio of thermal diffusion time to insertion time be large. Further, the temperature sensitive materials exhibit an irreversible behavior which means that only one experimental run can be made per coating. Finally, since the technique is transient, motion pictures must be taken of each experiment. This could become prohibitively expensive if one wishes to conduct parameter studies.

The aerodynamic studies of Klein [34, 35] employed unencapsulated cholesteric liquid crystals as the surface temperature sensor. The primary objective of Klein's work was to evaluate the feasibility of using liquid crystals to determine the location of the laminar and turbulent boundary layers that develop on wind tunnel aircraft models. The unencapsulated liquid crystals were applied directly to the model surface and, at the appropriate conditions of free stream air temperature and velocity, the portion of the model that was wetted with a turbulent boundary layer

exhibited a different color than its laminar counterpart. The difference in color displayed by the liquid crystals resulted from the slightly higher adiabatic wall temperature associated with the turbulent flow. Although Klein was able to obtain such qualitative information using the liquid crystal technique, he was unsuccessful in attempts to obtain accurate quantitative data due to the adverse effects that surface contamination, ultraviolet light and flow induced shear stress produced on the unencapsulated liquid crystals. In a follow on study, Klein and Margozzi [39] attempted to develop a technique for visually measuring shear stress by utilizing the shear stress sensitivity of certain types of unencapsulated cholesteric liquid crystals. Although they found that liquid crystals could be formulated that were relatively sensitive to shear and insensitive to temperature, they found it difficult to accurately interpret the color signal produced by the crystals since the liquid crystal coating tended to flow and develop a rough texture in response to the shearing effects of the flow. It was concluded that while it appeared feasible to measure shear stress using unencapsulated liquid crystals much additional research would be needed to develop liquid crystals that would exhibit high shear sensitivity while at the same time maintaining low temperature, angle and pressure dependence.

McElderry [40], in an investigation similar in principle to the one conducted by Klein, used encapsulated cholesteric liquid crystals as a means of determining boundary layer transition on a flat plate placed in a supersonic air stream. McElderry found that the encapsulated liquid crystals produced color displays that were not affected by the adverse sensitivity to shear and contamination that Klein had experienced with the unencapsulated liquid crystals. McElderry also found that the colors displayed by the encapsulated liquid crystals were relatively independent of viewing angle.

The motivation for the present investigation was prompted by McElderry's success with the encapsulated liquid crystals. Because of the shear insensitivity displayed by the encapsulated liquid crystals, it was felt that it would be possible to develop a liquid crystal thermographic technique that would allow direct visual determination of both quantitative and qualitative heat transfer information on heated objects placed in forced convection environments. With this as the primary goal, the present investigation was undertaken.

III. EXPERIMENTAL APPARATUS

In the initial phase of this investigation, an acrylic tube wrapped with Nichrome ribbon was used as the test cylinder. This cylinder had been previously used by Meyer [6] in a study of the heat transfer characteristics of a uniformly heated cylinder placed in a crossflow of air. Several problems were encountered using the Nichrome wrapped cylinder and an improved experimental procedure was established using a cylinder constructed from an electrically resistive carbon impregnated paper that shall henceforth be referred to as "Temsheet." Final data were collected using the Temsheet cylinder as the experimental model.

Wind Tunnel

The experimental study was carried out using a low speed Aerolab wind tunnel with a test section that was 81 cm high and 114 cm wide. The tunnel had a four speed transmission and was powered by a 100 hp electrical motor. The motor was capable of generating a maximum speed of 90 m/sec with a clear test section. With the cylinder in the test section, however, the peak speed was 77 m/sec. The turbulence intensity of the wind tunnel was measured using a Thermo-Systems hot wire anemometer and its associated electronic equipment. The turbulence intensity, which was measured in the

clear test section, ranged from 0.5% to 0.7% over the range of speeds of interest.

Nichrome Wrapped Cylinder

The test cylinder initially employed in the investigation was constructed from an acrylic tube. It was 81 cm long and spanned the entire height of the wind tunnel test section. It's 11.35 cm diameter and 0.76 cm wall thickness were the final dimensions after being machined into round. The choice of a relatively large cylinder diameter permitted sufficiently large Reynolds numbers for examining both subcritical and critical flow regimes.

A circuit for generating a constant heat flux on the surface of the cylinder was installed by helically wrapping Nichrome ribbon around the circumference of the cylinder. The Nichrome ribbon was 0.95 cm wide and 0.008 cm thick, and exhibited an electrical resistance of 0.015 ohms per cm of length.

To facilitate the wrapping process and to promote a smooth surface, the cylinder was grooved one thread per cm, 0.95 cm wide and 0.013 cm deep. This left a separation of only about 0.063 cm between individual wraps, giving a close approximation to a uniformly heated surface. The ends of the ribbon were led through slots from, and back into, the interior of the cylinder where they were connected to power leads. The ribbon was bonded to the cylinder with RTV-108 silicone rubber adhesive.

The main circuit consisted of 39 wraps and had a total resistance of 20.527 ohms. Variations in this resistance due to temperature changes were negligible. As shown in Figure 1, the main circuit was located approximately in the center of the cylinder, beginning 23.1 cm from the base and extending 38.4 cm up the length of the cylinder. A uniform surface heat flux was generated by passing a known current through the main circuit. Two smaller

guard heater circuits were installed above and below the main circuit. These consisted of three wraps of Nichrome ribbon whose ends were led through separate slots. Each pair of guard leads was connected to a separate power supply. This arrangement allowed the guard heater circuits to be controlled individually. The test section, which was designated as the center wrap of the main circuit, was instrumented with four copper-constantan thermocouples attached at 90 degrees intervals as shown in Figure 1. Four additional thermocouples were used to control the guard heaters. Two of these were located on the center wrap of the guard circuits. The remaining two thermocouples were located near the edges of the main circuit and provided the comparative temperature information required for the guard heater system to function.

Two static pressure pickups were installed in the cylinder wall as shown in Figure 1. These were made of 0.1 cm (o.d.) stainless steel tubing, and had an orifice of 0.08 cm (i.d.). In this way, surface pressure was measured and input to one side of a U-tube water-filled manometer. The manometer was referenced against the static pressure at the entrance of the test section.

After the thermocouples and pressure taps were in place, the cylinder was filled with Silastic, S-5370, RTV foam, a low density resilient silicone rubber. The foam was easily poured into the cylinder and quickly expanded, uniformly filling every crevice.

The foam proved to be an excellent thermal insulator, exhibiting a thermal conductivity of approximately 10^{-4} cal/cm $^{\circ}$ C-sec. Unfortunately, a serious disadvantage of the foam was its large thermal capacity which considerably increased the delay before reaching steady state conditions. Long experimental runs were the outcome of this objectional feature.

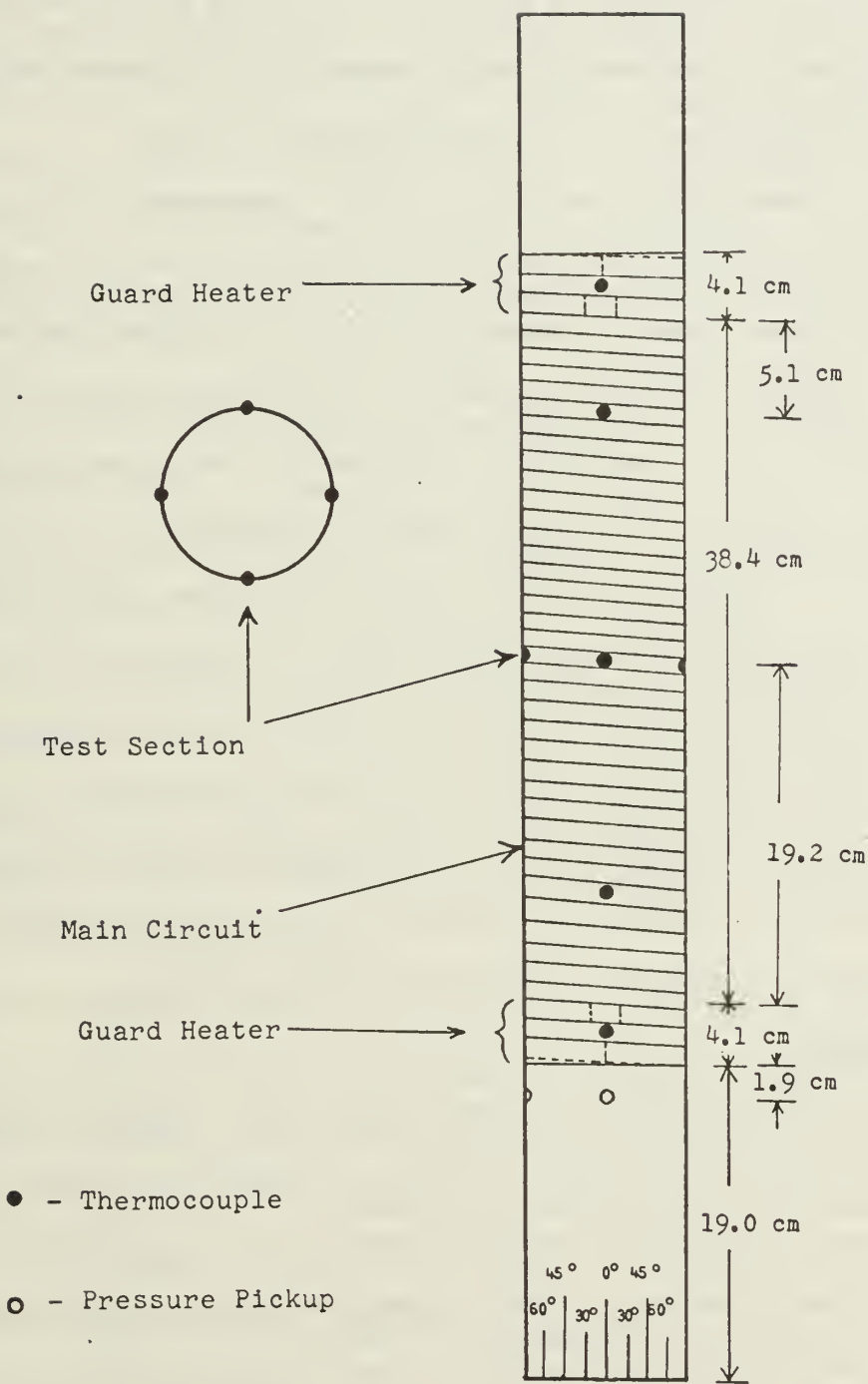


Figure 1 Schematic of Nichrome cylinder.

The cylinder was mounted on a turntable base that could be rotated from outside the wind tunnel. A disk that was marked every five degrees rotated with the cylinder base allowing temperature difference and surface pressure to be determined at any desired angular location.

Prior to embarking on the liquid crystal thermographic study, the Nichrome wrapped cylinder instrumented with thermocouples was used to investigate the heat transfer characteristics of a uniformly heated cylinder placed in a crossflow of air. The details of that investigation can be found in reference [6]. The initial experimental plan called for use of the Nichrome cylinder to obtain heat transfer information using both the thermocouple technique and the liquid crystal technique. The data obtained using the liquid crystal technique were then to be compared to the data collected with the thermocouples to gain a feeling for the accuracy of the liquid crystal technique. This objective was only partially accomplished for as our experiments progressed it became apparent that the large surface irregularities which continued to develop on the Nichrome wrapping were producing large uncertainties in the heat transfer results.

Temsheet Cylinder

A test cylinder that did not exhibit the large surface irregularities displayed by the Nichrome wrapped cylinder was constructed from a commercially produced, electrically resistive paper known as Armstrong Temsheet. Temsheet is a thin, flexible, carbon impregnated paper containing no wires or ribbons. The nominal thickness is 0.1 cm and the electrical resistivity is approximately 2.5 ohm-cm. The heat that is generated when a constant electrical current is passed through a square section of the paper is uniform to within 2% from point to point.

A hollow cylinder, with an outer diameter of 10.0 cm and a length of 30.0 cm, was formed from a section of Temsheet. Prior to forming the Temsheet into a cylindrical form, two strips of aluminum tape were attached in parallel fashion to what was to be the inner surface of the cylinder. One of the aluminum strips was placed 7.5 cm down from the top of the Temsheet section and the other was placed 7.5 cm up from the bottom. This left a 15 cm region between the strips. By attaching power leads to the aluminum strips, the strips were made to serve as electrodes. A uniformly heated test section was established by passing a constant electrical current between the aluminum strips and the Temsheet, a silver based conductive paint was applied along the inner edges of the strips.

To guard against free convection effects in the internal region of the Temsheet cylinder, the cylinder was tightly packed with glass wool. The glass wool also added a degree of structural rigidity to the cylinder and aided in resisting deformation when an external velocity field was applied around the cylinder.

The Temsheet cylinder was supported in the central section of the wind tunnel with the aid of two wooden end pieces. These end pieces were 10.0 cm in diameter, 30 cm long, and were permanently attached to the floor and ceiling of the wind tunnel. The end piece attached to the floor of the wind tunnel had a 3.0 cm hole drilled through its axis through which electrical leads could be passed. The last 5.0 cm on each end piece was turned down approximately 0.125 cm. This small step in each end piece allowed the Temsheet to be smoothly and firmly attached to the wood with double backed tape.

The completed assembly presented a smooth, continuous cylinder, 81 cm in length and 10.0 cm in diameter, to the flow. Only the center 15 cm

of the Temsheet cylinder, however, was heated. No guard heating was employed in this design. An elementary heat transfer analysis [41] indicated that edge effects were significant only to within approximately 1 cm of each electrode. As such, data were collected only within the central 10 cm of the 15 cm heated section.

IV. LIQUID CRYSTAL APPLICATION AND CALIBRATION

Application

The temperature distribution around the circumference of the Nichrome wrapped cylinder was obtained by attaching tapes coated with encapsulated liquid crystals around the circumference of the cylinder. A number of tapes, each coated with a liquid crystal formulation that responded to a different temperature, were attached at various axial locations on the cylinder. Although it is possible to obtain commercially made liquid crystal tapes, the tapes employed in the present set of experiments were made by spraying Testor's flat black paint onto 2.5 cm wide Scotch double coated tape, #404. Encapsulated liquid crystals, in slurry form, were then applied to the blackened surface with the aid of a small brush. Two coats of liquid crystals were applied. The entire composite was then sealed with a coating of polyurethane. This procedure yielded a composite that was approximately 0.020 cm thick. Of this total thickness, approximately 0.008 cm was due to the liquid crystal coating.

Applying the liquid crystals to the Temsheet cylinder proved to be far easier and less time consuming than the procedure required for the Nichrome wrapped cylinder. Since the Temsheet cylinder was black, there was not need to apply black paint to the surface. Further, due to the paper-like texture of the Temsheet, it was possible to apply the liquid crystals directly to the surface of the Temsheet eliminating the need for

tapes. Two coats of the slurry based encapsulated liquid crystals were found to produce optimum color brilliance. Figure 2 is a photo taken through a scanning electron microscope of a piece of Temsheet partially coated with encapsulated liquid crystals. Careful inspection of the photo shows the liquid crystal coating to be composed of spheroids with diameters on the order of 20-50 microns. It is also interesting to note the surface texture of the Temsheet itself. Although smooth to the touch, it is seen that the material is quite fibrous in nature.

Calibration

A water filled, Rosemount constant temperature bath, capable of establishing and maintaining temperature to within 0.01°C accuracy, was employed in the liquid crystal calibration procedure. The bath temperature was monitored and controlled with a platinum resistance thermometer. The eye was used to determine color. All liquid crystal formulations were calibrated on a piece of the material to which they would be applied for data collection. The liquid crystal coated substrates were enclosed in small, clear plastic bags to seal them from the damaging effects of water. The package was then suspended in the water bath. The temperature of the bath was slowly raised until the event temperature range was reached. By carefully adjusting the bath temperature, an accurate measure of the event temperature corresponding first to the onset of red, then to green and finally to blue was made. No attempt was made to determine shades of red, green, or blue, simply their onset. The procedure was also reapeated in reverse order by slowly lowering the bath temperature through the event temperature range and noting the end of the blue, green and red displays. Using this procedure, temperature and color were calibrated to within an estimated accuracy of 0.1°C . Table 1 lists the calibration results. It

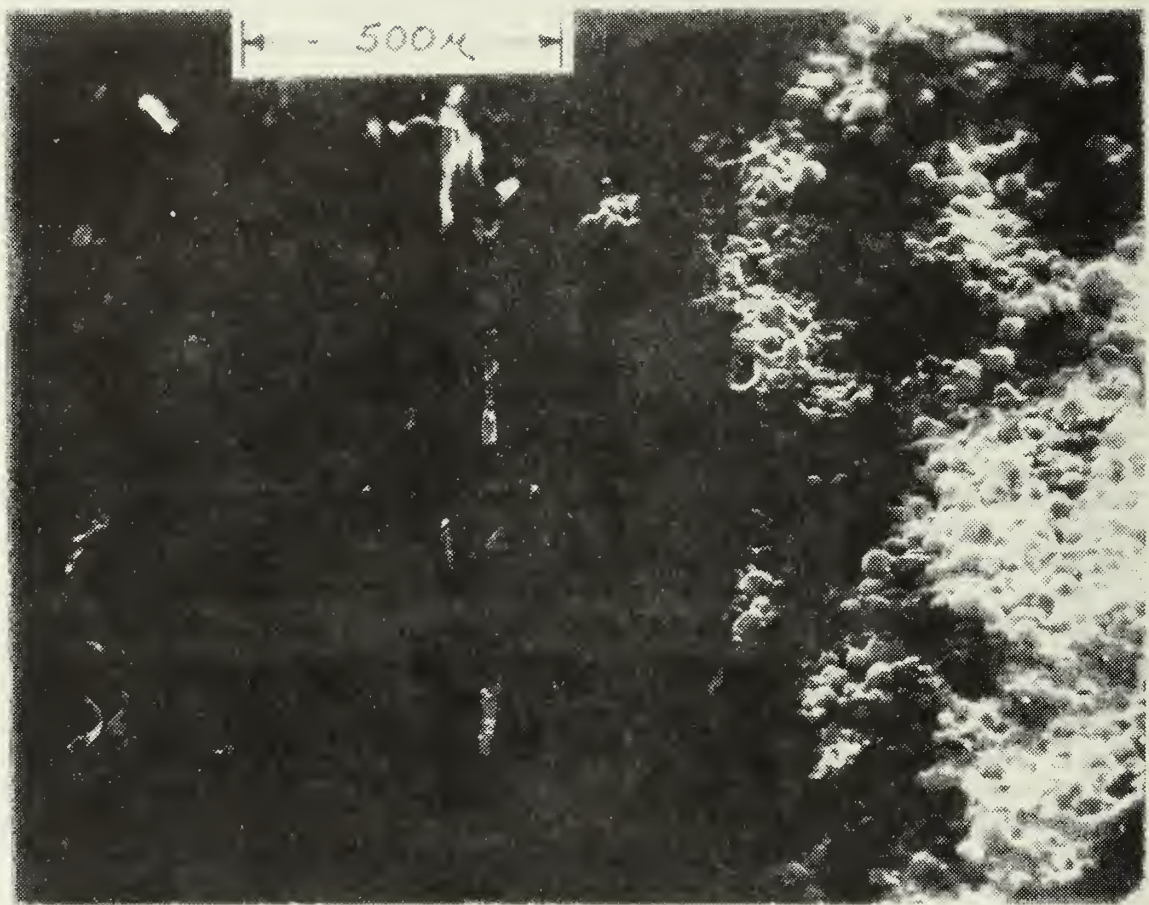


Figure 2 Photograph taken through an electron microscope of the Temsheet-liquid crystal interface.

should be noted that the observer who calibrated the liquid crystals also made all color determinations during the actual experimental runs.

Table 1

Liquid crystal calibration results. Temperatures listed refer to the onset of red, green, and blue, respectively.

| Liquid Crystal (NCR Designation) | Color Transition Red ($^{\circ}$ C) | Color Transition Green ($^{\circ}$ C) | Color Transition Blue ($^{\circ}$ C) |
|-------------------------------------|---|---|--|
| S-30 | 29.9 | 30.2 | 30.8 |
| S-32 | 32.5 | 33.1 | 33.7 |
| R-33 | 33.8 | 34.3 | 35.3 |
| S-34 | 34.7 | 35.1 | 35.7 |
| S-36 | 36.4 | 36.8 | 37.4 |
| R-37 | 37.2 | 37.6 | 39.1 |
| S-38 | 38.6 | 39.1 | 39.7 |
| S-40 | 40.6 | 41.1 | 41.7 |
| R-41 | 41.1 | 41.9 | 43.2 |
| S-43 | 43.2 | 43.9 | 44.6 |
| S-45 | 45.1 | 45.6 | 46.2 |
| R-45 | 42.7 | 43.3 | 44.5 |
| R-49 | 49.8 | 50.0 | 51.2 |

V. EXPERIMENTAL PROCEDURE

Nichrome Wrapped Cylinder

Initially, the temperature readings obtained using the liquid crystal tapes placed on the Nichrome wrapped cylinder were compared with the thermocouple readings. The procedure outlined by Meyer [6] was used to bring the cylinder to steady state conditions. It should be noted that the relatively large thermal capacity of the foam which filled the inside of the acrylic tube dictated a start-up transient on the order of 3 hours. Six liquid crystal tapes were attached to the cylinder. Starting from the uppermost liquid crystal tape and moving downward, the tapes were coated with the following liquid crystal formulations: R-49, S-45, R-45, R-41,

R-37, and R-33. Having reached steady state, the angular location of the red, green and blue transition points on each tape were noted. Thermocouple readings were then taken at the forward stagnation point and every 15 degrees of arc back to the rear stagnation point.

Due to the difference in location of the two types of temperature transducers, a slight difference was expected in the temperature readings indicated by the two. The thermocouples were attached to the inside of the Nichrome ribbon while the liquid crystals were on the surface of the tape. As such, a conductive resistance separated the two. An elementary heat transfer analysis [41] indicated that a temperature difference on the order of 1°C would exist between the two sensors. This indeed proved to be the case. The tape coated with liquid crystal R-45 was located directly over the portion of Nichrome ribbon which was instrumented with the thermocouples. The thermocouples acted as heat sinks and were easily found during the warm-up period of the cylinder. By adjusting the power applied to the Nichrome ribbon, a color transition could be forced to occur directly over a thermocouple. When tape R-45 appeared red (42.7°C), the thermocouple indicated a temperature of 43.2°C . At the green (43.3°C) and blue (44.5°C) color transition points, the thermocouple read 44.1°C and 45.3°C , respectively. The difference between the two sets of readings varied from 0.5° to 0.8°C . Since this difference was close to the predicted temperature drop across the conductive resistance, it was concluded that liquid crystal tape R-45 was yielding accurate temperature information.

Unfortunately, it was not possible to accurately check the validity of the temperature readings provided by the remaining 5 liquid crystal tapes. As can be seen in Figure 3, large surface irregularities existed on the surface of the cylinder. These surface irregularities caused local hot

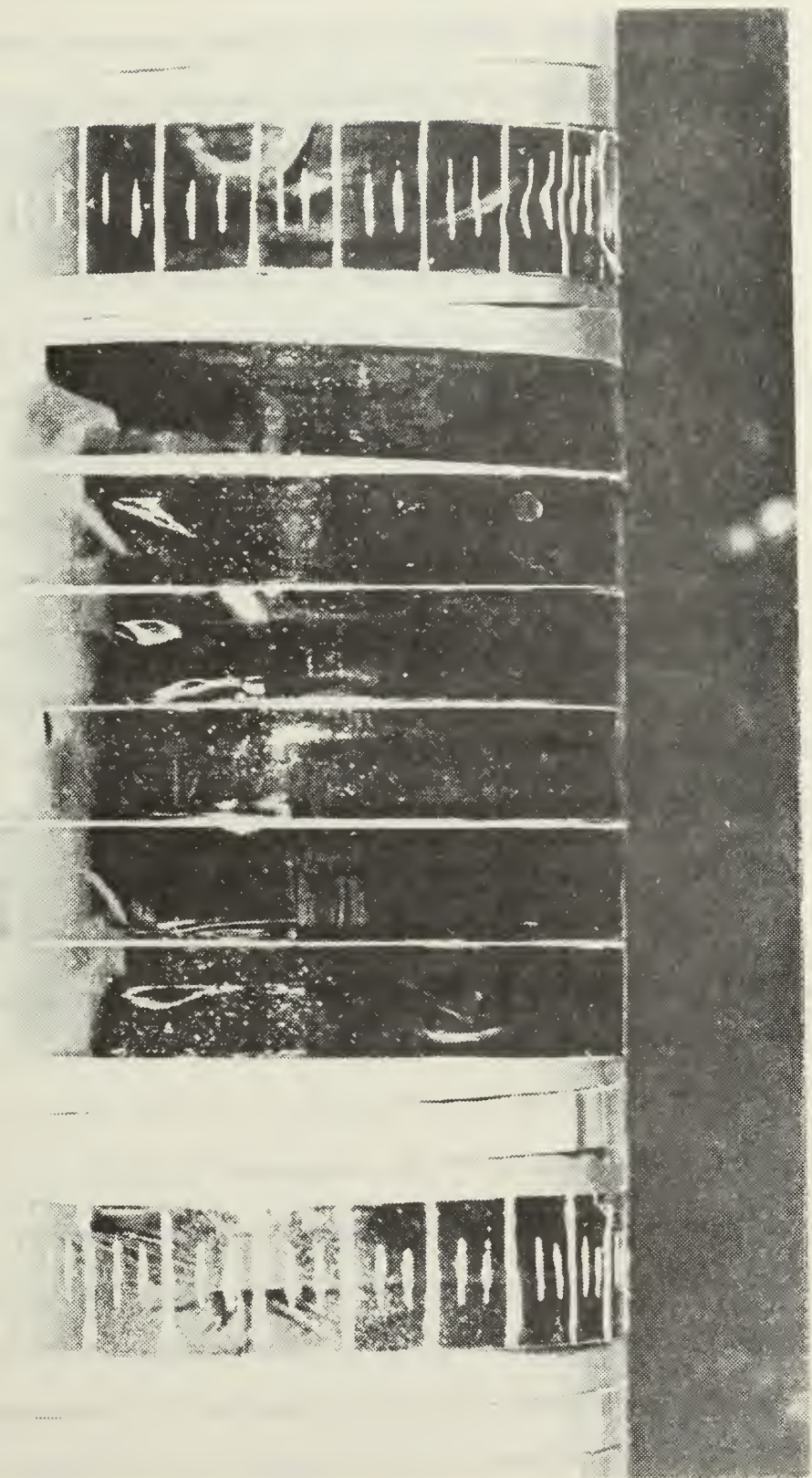


Figure 3 Nichrome-wrapped cylinder instrumented with the liquid crystal tapes. Note the presence of large surface irregularities.

and cold spots to develop. These spots were easily seen while the cylinder was warming up or when the cylinder was energized with no air flow. Further, due to the surface protuberances, the flow pattern appeared to be drastically altered. Local regions of turbulence appeared to be produced near the surface of the cylinder in regions that would normally be associated with laminar flow (0 to 80 degrees). These regions were visible as small regions of pulsating liquid crystal colors directly behind the irregularity. To further complicate matters, the number of surface irregularities increased as the number of heating and cooling cycles increased. The result of these irregularities was that a generator of the cylinder could not be considered to be a line of flow or temperature constancy. As such, a temperature recorded with a thermocouple at a given axial and angular location could not be assumed to apply to the same angular location at a different axial location. Seban [5] experienced a similar problem with surface irregularities when studying the influence of turbulence on the heat transfer characteristics of a Nichrome wrapped cylinder.

The three dimensionality of the flow field, and resultant two dimensionality of the surface temperature distribution produced by the surface irregularities which developed on the Nichrome ribbon, prompted the design of the Temsheet cylinder. It should be noted, however, that the two dimensionality of the temperature field did not preclude the use of the liquid crystal thermographic technique. On the contrary, the liquid crystals gave a vivid display of the isotherm positions. However, one of the primary objectives of the investigation was to compare heat transfer data obtained with the liquid crystal thermographic technique with existing, accepted heat transfer results on a uniformly heated right circular cylinder placed in crossflow. In order to be assured that the experimental

conditions would be consistent with those maintained by others, it was necessary to employ a surface that was free of the large irregularities exhibited by the Nichrome.

Temsheet Cylinder

A cylinder constructed of Temsheet was used to develop a consistent method for obtaining accurate heat transfer data with the liquid crystals. Two different Temsheet cylinders were employed in this phase of the investigation. Both cylinders were of the design discussed previously. One Temsheet cylinder was coated only with liquid crystal S-43. This coating covered the entire 15 cm test section. The other Temsheet cylinder was coated with a series of circumferencial strips of liquid crystals. The strips were approximately 1 cm wide and were separated by 0.3 cm. The strips were located in the central 10 cm of the 15 cm test section. Figure 4 shows a photograph of the cylinder coated with the liquid crystal strips. As can be seen in the photo, reference marks were placed on the cylinder at 5 degree intervals. This greatly facilitated data taking. Reading in order from top to bottom, the following liquid crystal formulations were applied to the cylinder: R-49, S-45, S-43, S-40, S-38, S-36, S-34, and S-32.

Before proceeding with a description of the experimental procedure employed with the Temsheet cylinders, a brief qualitative description of the temperature distribution that exists on the surface of a uniformly heated cylinder placed in crossflow will be given. This description will prove helpful in describing and interpreting the liquid crystal results.

Flow past a cylinder may be classified as subcritical, critical, supercritical or transcritical. Roshko [42] presents an excellent discussion of the fluid flow phenomena associated with the various flow regimes. Since

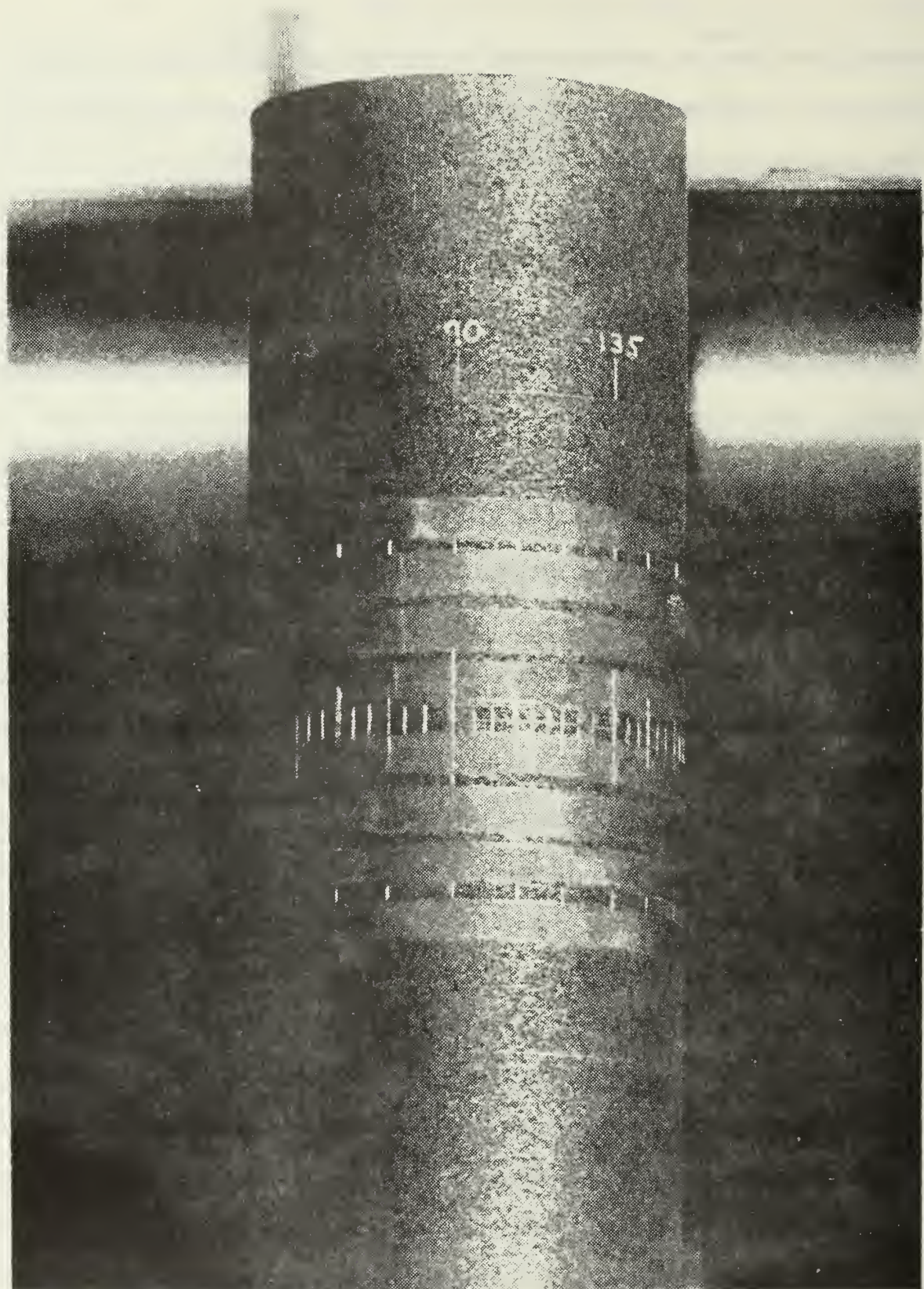


Figure 4 Photograph of the Temsheet cylinder coated with the eight liquid crystal bands. The colors displayed by the liquid crystals appear as the light gray regions in the black and white photo.

the present set of experiments examined Reynolds numbers ranging only from approximately 40,000 to 150,000, only the subcritical and critical flow regimes will be discussed here.

In subcritical flow, laminar hydrodynamic and thermal boundary layers grow from a minimum thickness at the forward stagnation point on the cylinder to a maximum thickness at an angular location of approximately 80-85 degrees. At this location the kinetic energy of the fluid in the boundary layer has been attenuated sufficiently due to frictional effects that the developing adverse pressure gradient can no longer be overcome. As a result, the laminar boundary layer separates and a turbulent wake develops.

Figure 5 depicts a typical subcritical flow pattern and the resulting trends in both temperature and heat transfer coefficient on the surface of a uniformly heated cylinder. Note that the maximum temperature exists at the separation point. This corresponds to the point of maximum thermal resistance, or minimum heat transfer coefficient. The ever decreasing temperature profile on the rear side of the cylinder is due to the scrubbing action of the highly turbulent wake. It certainly must be noted that the temperature profile depicted in Figure 5 on the rear side of the cylinder is an average profile. The actual profile is highly transient in nature due to the continually changing flow pattern in the wake.

Critical flow is characterized by the growth of a laminar boundary layer on the forward half of the cylinder just as in the subcritical flow case. The laminar boundary layer separates in the region of 80-85 degrees but, unlike the subcritical flow case, a subsequent transition to turbulent state of flow occurs resulting in the reattachment of a now turbulent boundary layer. This reattached turbulent layer ultimately separates at a position downstream of the laminar separation point. The region between

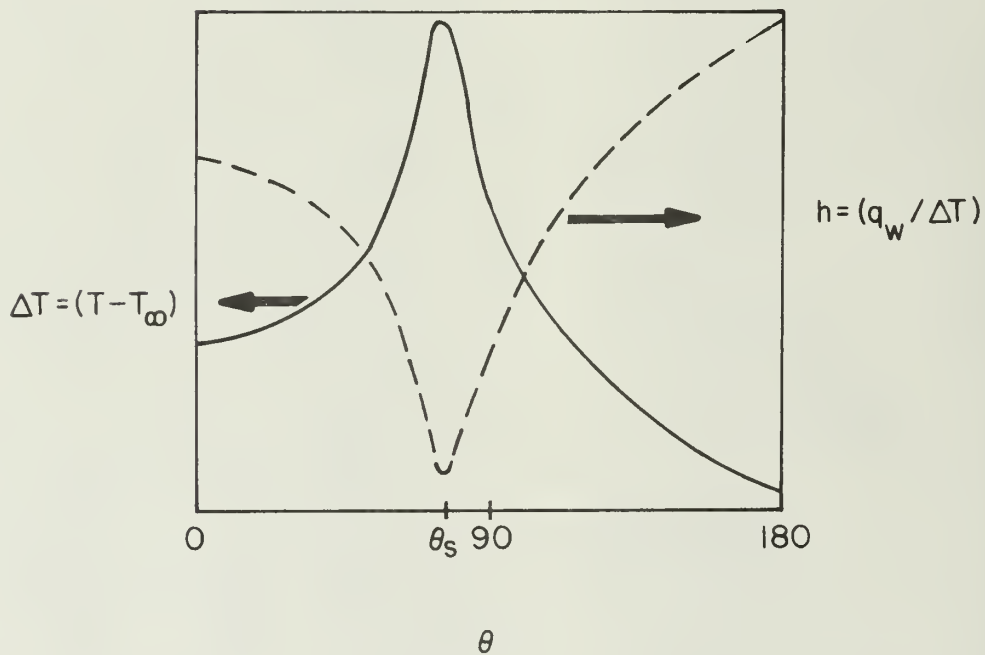
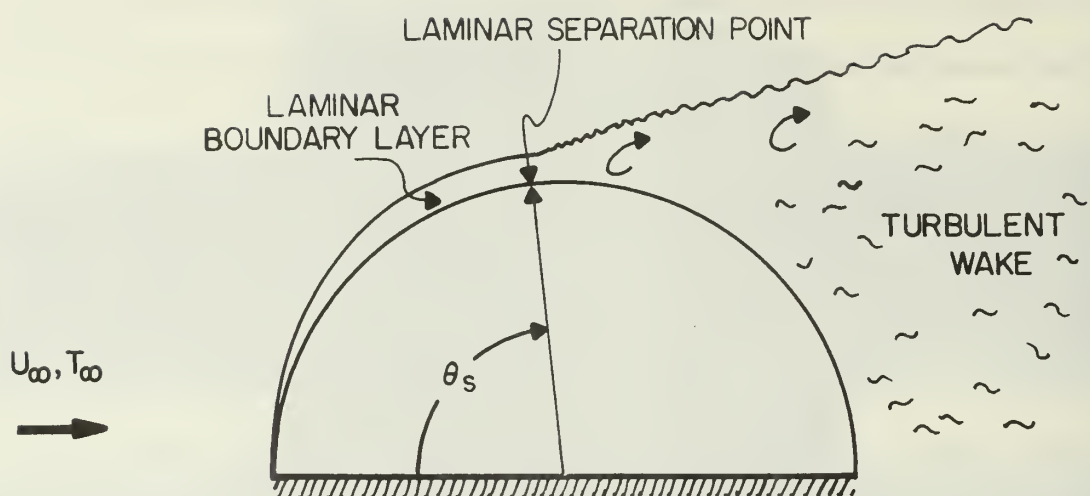


Figure 5 Sketch of a typical temperature distribution, T , that develops on the surface of a uniformly heated cylinder that loses heat in an amount q_w to a fluid stream. The fluid is at a uniform temperature, T_∞ , and is moving with velocity U_∞ . The conditions depicted are for subcritical flow as evidenced by the presence of a laminar separation at an angle θ_s .

the laminar separation point and the point of reattachment of the turbulent boundary layer is sometimes referred to as a "separation bubble" [42-44].

Figure 6 depicts a typical critical flow pattern and the resulting trends in both the temperature and heat transfer coefficient. Note that unlike the subcritical flow case, there are now two local temperature maxima. These exist at the location of the laminar and turbulent separation points. The local minimum in temperature which occurs between the two temperature peaks marks the point of reattachment of the turbulent boundary layer.

For data collection, the Temsheet cylinder with eight liquid crystal bands was installed in the wind tunnel. A reference thermocouple was placed upstream of the cylinder and was used to monitor air temperature. Air speed was monitored using a micromanometer that was attached in differential fashion to static pressure taps in the settling chamber and test section. The technique suggested by Pope [45] was used to correct the measured free stream velocity for the effects of solid blockage and wake blockage due to the presence of the model in the wind tunnel. Details can be found in [6] and [41]. For the case of the Temsheet cylinder, the correction amounted to less than 3%.

Prior to starting the wind tunnel, the electrodes on the inner surface of the Temsheet cylinder were attached to a power supply. The power supply was energized and voltage was adjusted to bring the surface temperature of the cylinder to a temperature of approximately 50°C. This caused all of the liquid crystal bands to pass through their event temperature ranges. Pre-heating the cylinder prior to initiating flow served three purposes. First, it allowed the resistance of the 15 cm test section to be measured at conditions of maximum expected temperature. It was found that the

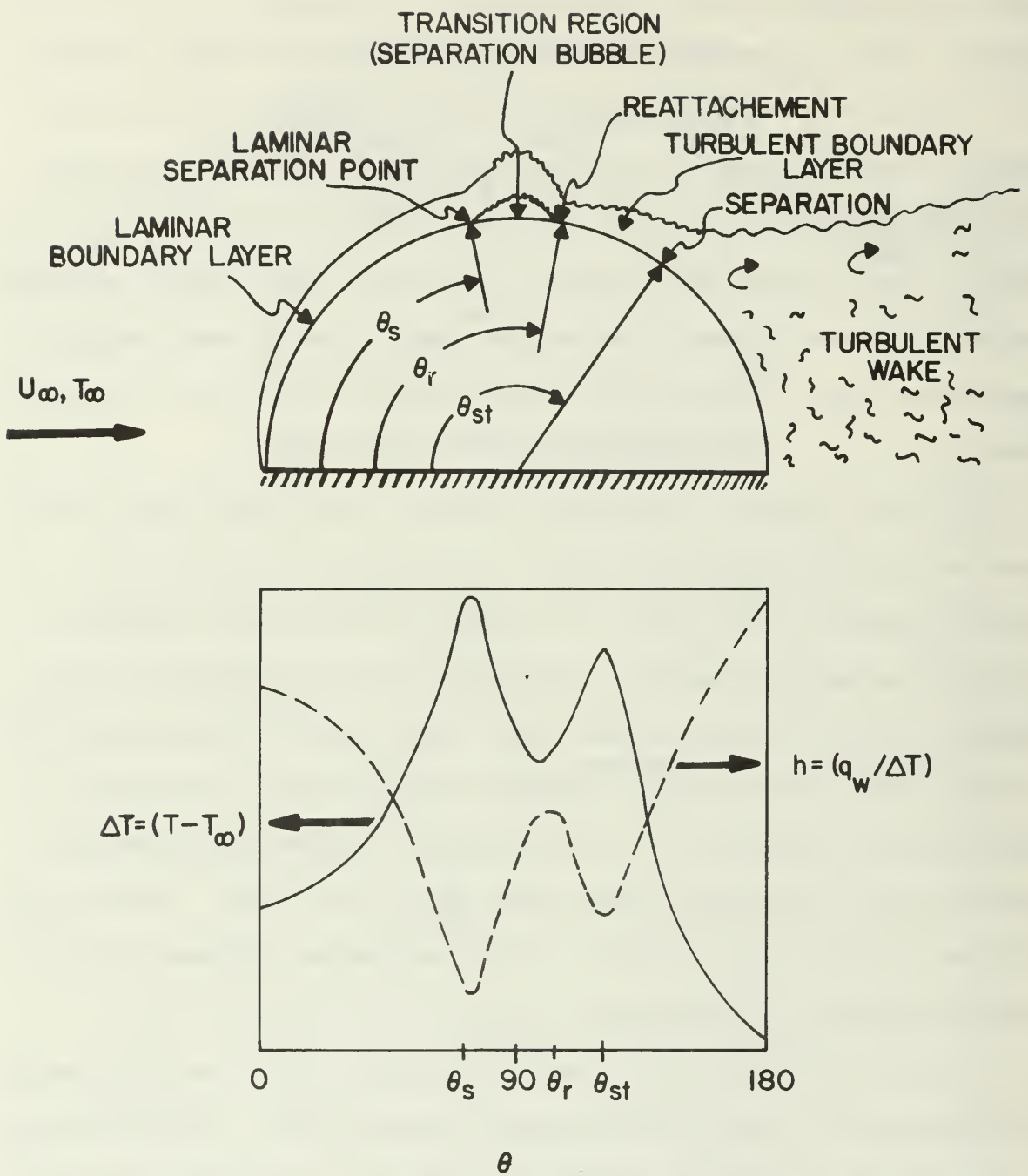


Figure 6 Sketch of a typical temperature distribution, T , that develops on the surface of a uniformly heated cylinder that loses heat in an amount q_w to a fluid stream. The fluid is at a uniform temperature, T_∞ , and is moving with velocity U_∞ . The conditions depicted are for critical flow as evidenced by the presence of a laminar separation at an angle θ_s , a separation bubble region, a point of reattachment of a turbulent boundary layer at an angle θ_r , and a subsequent separation of the turbulent boundary layer at an angle θ_{st} .

resistance was 12.0 ohms. This was within 0.1 ohms of the room temperature resistance. Second, it allowed the uniformity of packing of the glass wool filling the inner portion of the cylinder to be checked. Regions of non-uniform packing showed up as local hot and cold spots on the surface of the cylinder. These regions were adjusted prior to initiating flow. Finally, pre-heating the cylinder reduced the time necessary to reach steady state once the tunnel was started.

Having pre-heated the cylinder, flow was established in the wind tunnel. Immediately after flow was initiated, the cylinder started to cool. To counter this, the power supplied to the cylinder was increased to maintain the hottest spot on the cylinder at 49.8°C . This corresponded to the red transition point on liquid crystal R-49. Referring to Figures 5 and 6, it is seen that the hottest point on the cylinder occurs at the point of laminar separation. In the range of Reynolds numbers studied in the present investigation, 40,000 to 150,000, this point varied from 81 to 87 degrees. This is consistent with the location of laminar separation points found by others [46].

Power was continually adjusted to maintain liquid crystal R-49 red at the laminar separation point until steady state conditions were reached. This usually occurred within fifteen minutes after flow was initiated in the tunnel. At least 5 minutes were allowed beyond the time at which steady state was judged to have been reached before data were collected.

It was found that the most accurate temperatures were found at the beginning of the color transitions of the liquid crystals. In the regions where temperature gradients were sharp, there was no problem in visually determining the onset of the red, green and blue transitions. The particular liquid crystal in the temperature range at these locations would undergo

the red to green to blue transitions over a short distance. The point of blue transition was particularly easy to locate.

The point of color transition near the forward and rear stagnation points of the cylinder was much more difficult to locate. The temperature gradients in these regions were quite shallow, particularly in the forward stagnation region. It was not uncommon for a given liquid crystal to exhibit approximately the same color over 15 to 20 degrees of arc. The actual transition to a particular color usually was not apparent. The uncertainty in interpreting temperature by color in such regions was on the order of 0.5°C . This was improved on by adjusting the power level to force a color transition in the particular region of interest.

For critical flows, the procedure for locating separation was followed to locate the points of laminar separation, reattachment and turbulent separation. The separation bubble manifested itself as a local cool spot bounded by two local hot spots. In the present set of experiments, such a cool region first appeared at a Reynolds number of 121,500. This marked the onset of critical flow conditions. Only two critical flow Reynolds numbers were examined, 121,500 and 148,000. At larger Reynolds numbers, visible deformation occurred at the forward stagnation region on the cylinder.

Precise temperature data were not obtained using the cylinder coated entirely with liquid crystal S-45. This cylinder was used only to test for edge effects and the straightness of the isotherms in the axial direction.

VI. RESULTS

Temperature Distribution

Figures 7 and 8 are sketches of typical liquid crystal displays associated with subcritical and critical flows, respectively. Figure 4 is

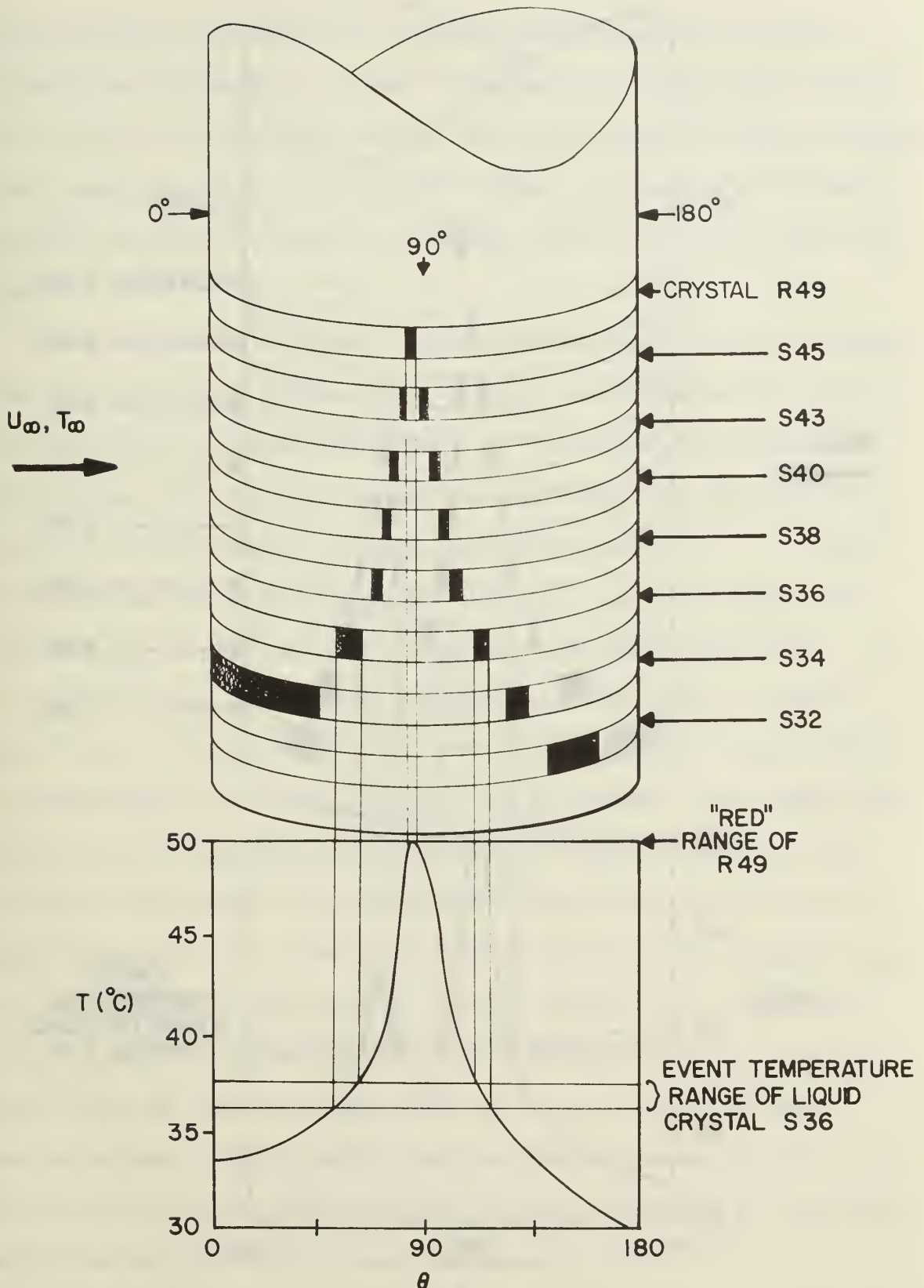


Figure 7 Schematic of a typical liquid crystal display. The conditions depicted are representative of subcritical flow. The shaded regions on each liquid crystal band represent color.

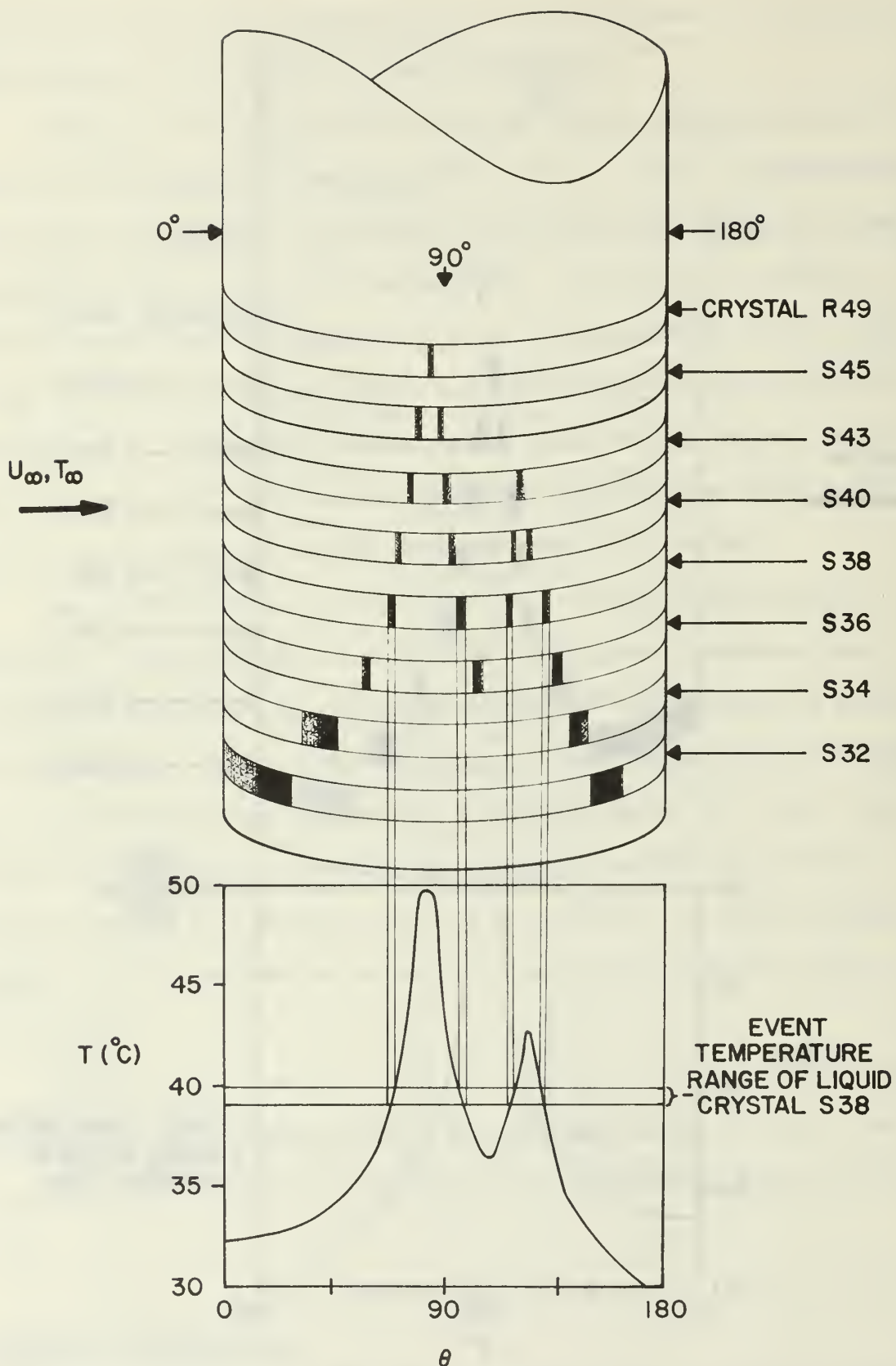


Figure 8 Schematic of a typical liquid crystal display. The conditions depicted are representative of critical flow. The shaded regions on each liquid crystal band represent color.

a black and white reproduction of a colored photo taken of the heated cylinder placed in subcritical flow. Although color is not evident in the photo, on close inspection one can see small gray regions similar in location to the shaded regions shown in Figure 7. These gray regions are the color bands that are clearly evident to the naked eye and in colored photos and movies.

The sketch shown in Figure 7 depicts the case where the power supplied to the test section has been adjusted to force liquid crystal R-49 to turn red at the point of laminar separation. At this particular power level, liquid crystal S-45, which is located just below R-49, has been heated in excess of its event temperature range along the separation line. However, just forward and aft of the separation line the cylinder has been cooled sufficiently by the flow to be in the event temperature range of S-45. As such, the S-45 strip displays two separate regions of color. A similar pattern exists on strips S-43, S-40, S-38 and S-36, but the spacing between the colored regions continually widens. Due to the very mild surface temperature gradient that exists near the forward stagnation region on the cylinder, liquid crystal S-34 is depicted as displaying color over a very large arc length. As has been previously discussed, precise color interpretation was difficult in this region. Liquid crystal S-32 is depicted as displaying only one colored region. This is because the region of the cylinder near the rear stagnation point was normally cooled to lower temperatures than a similar region near the forward stagnation point. As such, the entire forward portion of the cylinder is depicted as existing at temperatures greater than the event temperature of S-32.

The sketch shown in Figure 8 again depicts the case where the power supplied to the test section has been adjusted to force liquid crystal R-49

to turn red at the point of laminar separation. As can be seen, the entire surface of the cylinder, with the exception of the laminar separation line, exists at temperature below the event temperature of R-49. Liquid crystal S-45 again yields color displays at two locations as was the case in subcritical flow. For the case of critical flow, however, liquid crystal S-43 has been depicted displaying three colored regions. A glance at the surface temperature distribution shown sketched just below the cylinder indicates why. Unlike the subcritical flow case, after the laminar boundary layer separates, a separation bubble develops followed by a subsequent reattachment of a turbulent boundary layer. The turbulent boundary layer thickens and ultimately separates producing the local temperature maximum indicated by S-43. The trend in the liquid crystal displays around the point of turbulent separation is identical to the trend in displays around the laminar separation point. Accordingly, liquid crystals S-40 and S-38 have been depicted as showing four distinct colored regions. Liquid crystal S-36, however, shows only three bands, the reason being that the event temperature of S-36 is the minimum temperature in the separation bubble, presumably the point of reattachment of the turbulent boundary layer.

Figures 7 and 8 have been presented for the purpose of explaining the significance of typical liquid crystal displays. Various other displays were produced by adjusting the power supplied to the test section. By carefully controlling the power level, a particular liquid crystal could be forced to undergo a color transition at any desired location on the cylinder surface. This allowed the Nusselt number signature on the cylinder to be determined in a nearly continuous fashion without the necessity of rotating the cylinder.

It should be noted that just aft of the point of laminar separation, the surface temperature distribution was not steady. In the case of subcritical flows, the influence of the turbulent, scrubbing action of the wake was readily apparent. The colors displayed by the liquid crystals continually dimmed and glowed in response to the turbulence. Occasionally an isotherm would suddenly be shifted in position by several degrees of arc. A similar phenomena was observed in the wake of the cylinder in critical flow. Additionally in critical flow, the separation bubble region and the turbulent boundary layer also exhibited a degree of fluctuation. In contrast, the liquid crystal displays prior to separation appeared perfectly steady to the eye.

Local Nusselt and Froessling Numbers

The local wall heat flux was determined by dividing the power supplied to the cylinder test section by the surface area of the test section. The local heat flux was corrected for conduction and radiation effects using a technique similar to the one employed by Giedt [47]. The local convective heat transfer coefficient, h , was obtained by dividing the corrected local wall heat flux by the local surface temperature excess. The local Nusselt and Froessling numbers were then calculated in the standard form:

$$\text{Nusselt number, } \text{Nu} = hD/k$$

$$\text{Froessling number, } \text{Fr} = \text{Nu}/\sqrt{\text{Re}}$$

where

$$\text{Re} = \text{Reynolds number} = U_{\infty} D / v$$

D = Cylinder diameter

U_{∞} = Corrected free stream velocity

k = Thermal conductivity (film temperature)

v = Kinematic viscosity (film temperature)

Local Nusselt and Froessling numbers were obtained for Reynolds numbers ranging from 38,000 to 148,000. Several runs were made at higher Reynolds numbers, but the data were questionable due to the visible deformation that began to occur in the forward stagnation region of the cylinder at Reynolds numbers in excess of 150,000. Evidence of a separation bubble first appeared at a Reynolds number of approximately 121,500. As such, considering the effects of deformation, it was only possible to collect data on critical flow in the Reynolds number range 121,500 to 150,000.

Figure 9 is a plot of the angular variation of the Froessling number versus Reynolds number as determined with the liquid crystal thermographic technique. As can be seen, prior to separation the Froessling number is independent of the Reynolds number. An uncertainty analysis was conducted on the experimental results and it was found that the maximum uncertainty in determining the Froessling number occurred in the forward stagnation region. Using the method of Kline and McClintock [48], it was estimated that the experimental uncertainty in this region was 5%. The maximum uncertainty in determining the angular location of a particular isotherm was estimated to be 5 degrees of arc. Details of the uncertainty analysis can be found in reference [41].

Comparison with the Work of Others

The angular variation of the Froessling number obtained with the liquid crystal thermographic technique is compared with the experimental results of Giedt [4], Seban [5] and Meyer [6] in Figure 10. Also shown is a comparison of the present results with a theoretical prediction of the Froessling number variation. The theoretical curve was generated using the approximate technique recommended by Schuh [1]. Seban and Chan [2] and Perkins and Leppert [3] have also developed analytical models for

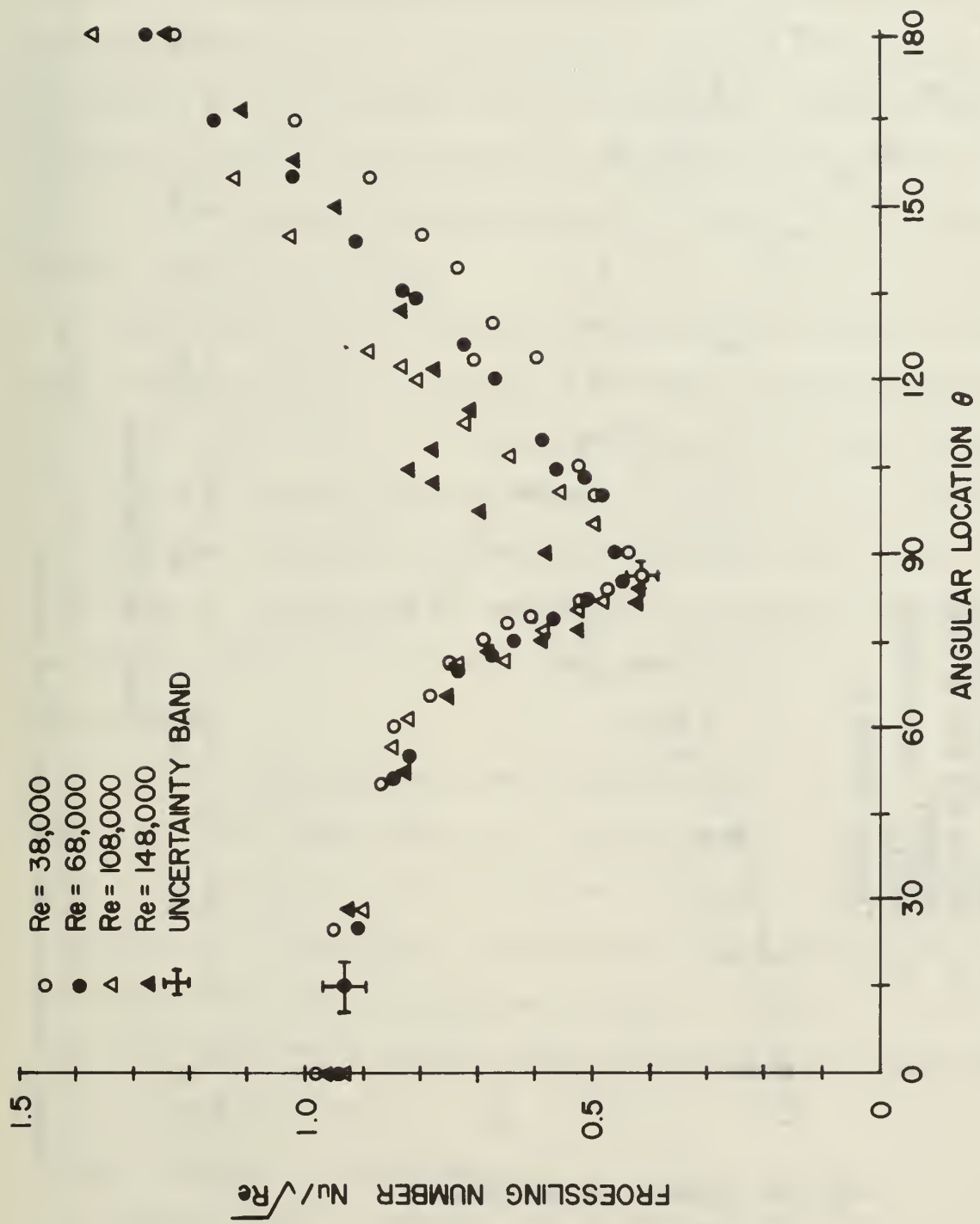


Figure 9 Experimental heat transfer results obtained using the liquid crystal thermographic technique.

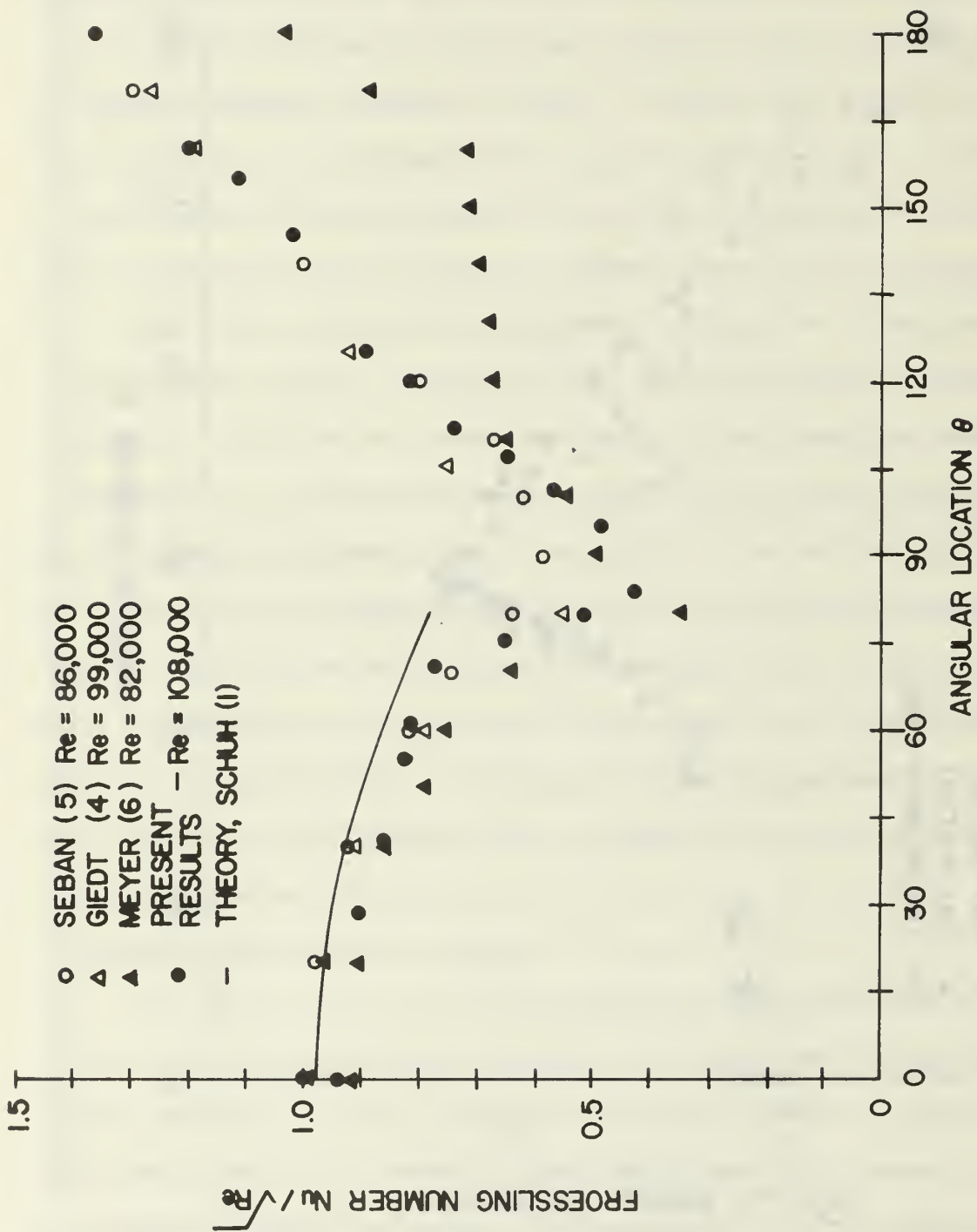


Figure 10 Comparison of the experimental heat transfer results obtained using the liquid crystal thermographic technique with the results of others.

predicting the heat transfer coefficient in the laminar flow region on a uniformly heated cylinder. All three models give approximately the same results. It is noted that beyond approximately 60° the experimental results and theory are no longer in good agreement. This was not unexpected. In the absence of actual pressure data on the Temsheet cylinder, an ideal pressure distribution was assumed in using Schuh's model. The use of the actual pressure signature could be expected to produce closer agreement between experiment and theory.

As can be seen, the agreement of the heat transfer results obtained with the liquid crystals is generally within the estimated experimental uncertainty when compared with the work of others. The results of Meyer present the one notable exception, especially in the wake region of the cylinder. As has been mentioned previously, however, large surface irregularities developed on the surface of the cylinder used by Meyer resulting in large uncertainties in Meyer's results.

Edge Effects

Figure 11 shows the isotherms that developed on the Temsheet cylinder coated only with liquid crystal S-43. As can be seen, the isotherms are vertical in the central region of the test section but tend to bend near the edges of the test section. The curvature of the isotherms near each electrode clearly indicates that heat is lost by conduction in these regions. These small edge effects were anticipated and data were not taken within 2.5 cm of each electrode.

Surface Roughness of the Temsheet

Figure 2 showed a magnified view of the liquid crystal-Temsheet composite. If the tiny, spherical shaped encapsulated liquid crystals are treated as surface roughness elements with average diameters of approximately

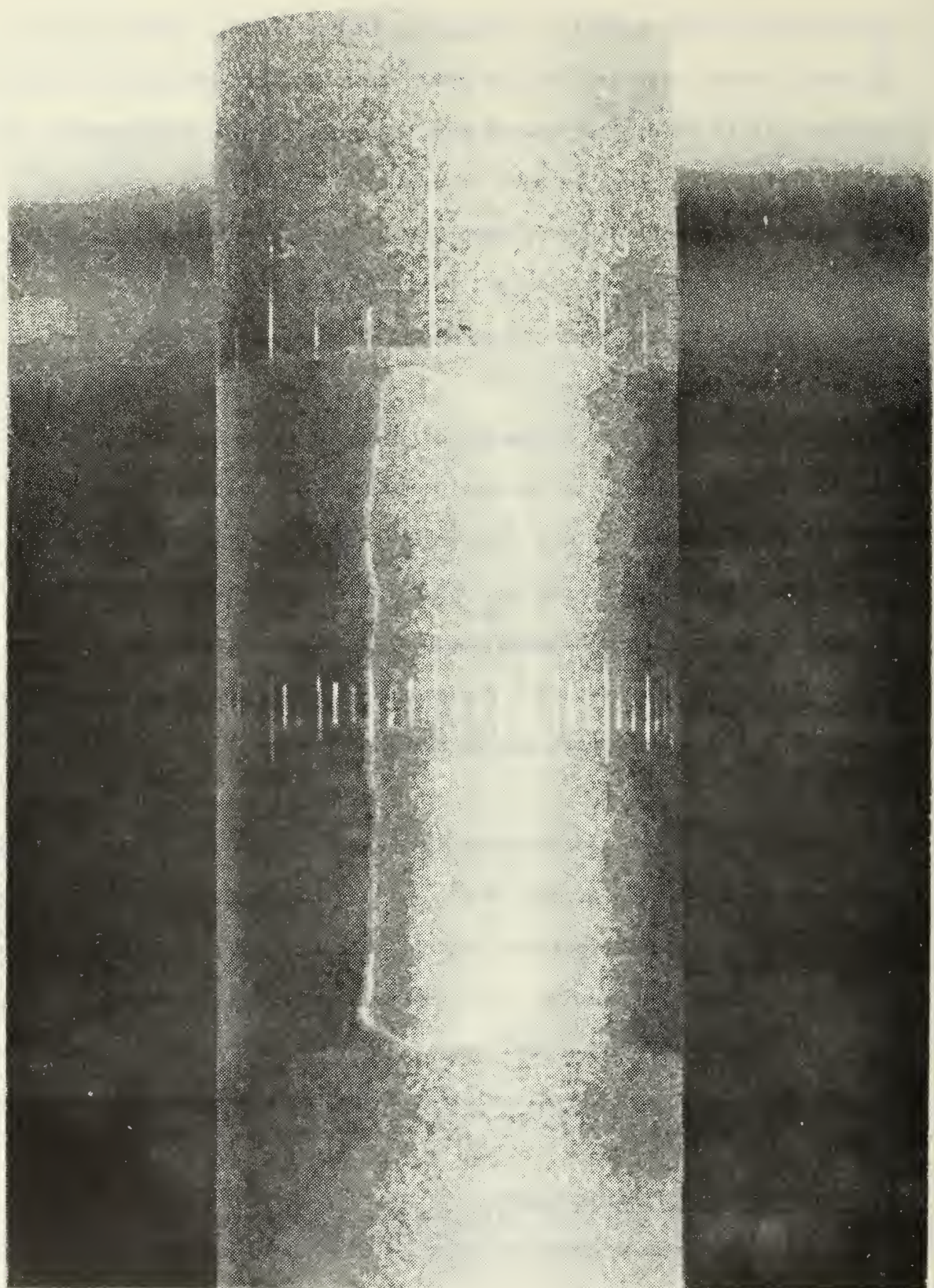


Figure 11 Photograph of the Temsheet cylinder coated only with liquid crystal S-43. The bending of the isotherms near the top and bottom of the test section indicates the influence of end losses on the temperature field.

35 microns, an estimate of the critical Reynolds number can be made. Achenbach [49] suggests in the case of spherical roughness elements on the surface of a circular cylinder that an equivalent sand gain roughness be calculated as $k = 0.55$ (diameter of spheres). In our case, $k/D = 20 \times 10^{-6}$. Using Achenbach's results for critical Reynolds number versus roughness, one finds that this represents a very smooth cylinder. The predicted critical Reynolds number is slightly in excess of 100,000. This is consistent with the value of 121,500 observed in the present set of experiments.

VII. SUMMARY

The liquid crystal thermographic technique developed in this investigation provides an excellent means of obtaining both qualitative and quantitative heat transfer information on heated objects placed in forced convection environments. Using the technique, it was possible to quickly and easily obtain information on the variation of the Nusselt number around the circumference of a uniformly heated right circular cylinder placed in a crossflow of air. The technique also allowed one to visually observe the effects of flow separation, the turbulent boundary layer, and the turbulent wake on the surface temperature of the cylinder. Colored movies taken of a cylinder coated with a single liquid crystal are especially vivid in their display of the influence of the turbulent wake on the cylinder surface temperature. In the wake region the liquid crystals continually dim and glow in response to the "scrubbing" action caused by random bursts of cool fluid impacting on a heated cylinder.

The ability to visually observe turbulent flow pattern effects on surface temperature suggests an excellent means for studying the influence of free stream turbulence on the heat transfer rates of heated objects.

However, in order that such a study be conducted in a quantitative manner, the thermal response time of the liquid crystals must first be determined. Fergason [50] estimated that the response time of a typical cholesteric liquid crystal film was on the order of 0.1 to 0.2 seconds. Parker [51], however, using a capacitor discharge technique and employing high speed photography, found that a 0.003 cm film of encapsulated cholesteric liquid crystals coated on a thin stainless steel foil responded in 0.036 seconds to a step change in the foil temperature. Parker also found that the response time of the liquid crystal coatings appeared to be thermal diffusion limited, increasing in proportion to the square of the thickness of the coating. It is possible that a thin coat of liquid crystals coated on a material such as Temsheet would respond even faster than a coating placed on a metal substrate due to the fact that the liquid crystals appear to be partially absorbed into the Temsheet. The ideal situation would be if the liquid crystals responded at the same rate as the Temsheet itself. An experiment, similar to the one conducted by Parker, needs to be conducted to determine the response time of the liquid crystals coated on a Temsheet substrate.

As a final recommendation, the phenomenon shown in Figure 12 is offered as a possible topic for future investigation. During the final phase of collecting wind tunnel data for the present investigation, it was noted that the cylinder coated with liquid crystal S-43 displayed alternate hot and cold spots along the separation line. These spots were uniformly spaced and seemed to be caused by some flow phenomenon, perhaps a series of vortices. Whatever the cause, the hot and cold spots definitely existed as is readily apparent in the photo. Precise measurements were not taken at the time the phenomenon was observed (the Reynolds number was

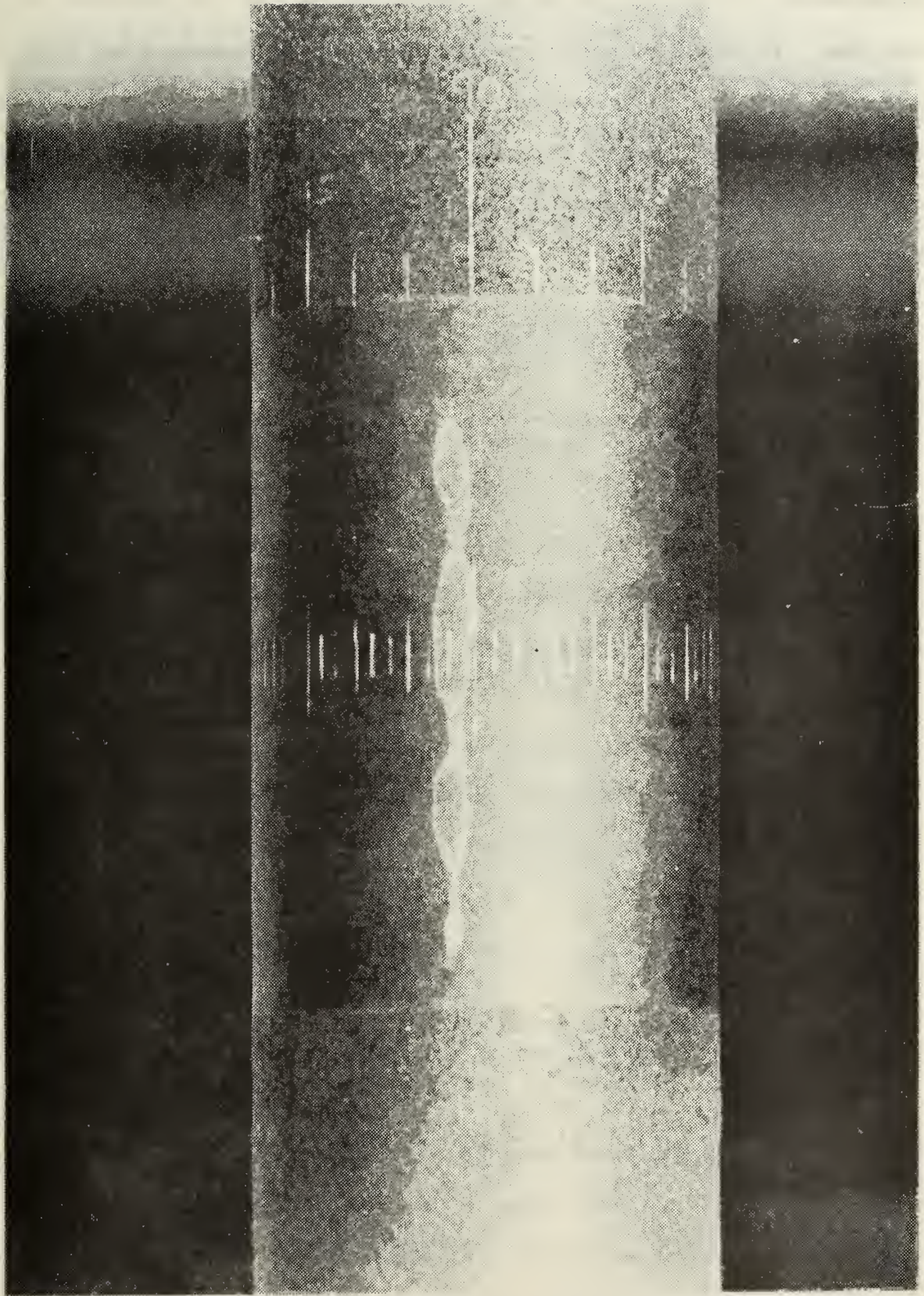


Figure 12 Photograph of the alternate hot and cold spots that developed along the separation line of the Temsheet cylinder.

approximately 75,000) and no explanation is offered for its existence at this time. It should be noted, however, that such a phenomenon may well have gone undetected if thermocouples were used as the temperature sensors. Additional research, perhaps using liquid crystals for temperature sensing and smoke for flow visualization, needs to be carried out to explain the observed phenomenon.

REFERENCES

1. Schuh, H., "A New Method for Calculating Laminar Heat Transfer on Cylinders of Arbitrary Cross Section and on Bodies of Revolution at Constant and Variable Wall Temperature," ASTIA, Ad 66184, 1953.
2. Seban, R. A. and Chan, H. W., "Heat Transfer to Boundary Layers with Pressure Gradients," ASTIA, AD 118075, 1958.
3. Perkins, H. C. and Leppert, G., "Local Heat Transfer Coefficients on a Uniformly Heated Cylinder," Int. J. Heat Mass Transfer, v. 7, 1964, pp. 143-158.
4. Giedt, W. H., "Effect of Turbulence Level of Incident Air Stream on Local Heat Transfer and Skin Friction on a Cylinder," J. of the Aeronautical Sciences, v. 18, 1951, pp. 725-730, 766.
5. Seban, R. A., "The Influence of Free Stream Turbulence on the Local Heat Transfer from Cylinders," J. Heat Transfer, Trans. ASME, v. 82, 1960, pp. 101-107.
6. Meyer, J. F., "An Experimental Investigation of the Heat Transfer Characteristics of a Heated Cylinder Placed in a Cross Flow of Air," Engineer's Thesis, Naval Postgraduate School, Monterey, Calif., June 1973.
7. Brown, G. H. and Shaw, W. G., "The Mesomorphic State: Liquid Crystals," Chem. Rev., v. 57, 1957, pp. 1049-1157.
8. Fergason, J. L., "Liquid Crystals," Scientific American, v. 211, no. 2, Aug. 1964, pp. 76-86.
9. Fergason, J. L. and Brown, G. H., "Liquid Crystals and Living Systems," J. Am. Oil Chem. Soc., v. 45, no. 3, March 1968, pp. 120-127.
10. Dreher, R., Meier, G., and Saupe, A., "Selective Reflection by Cholesteric Liquid Crystals," Molecular Crystals and Liquid Crystals, v. 13, 1971, pp. 17-26.

11. Kahn, F. J., "Cholesteric Liquid Crystals for Optical Applications," Applied Physics Letters, v. 18, no. 6, March 1971, pp. 231-233.
12. Castellano, J. A. and Brown, G. H., "Thermotropic Liquid Crystals: Part I. The Underlying Science," Chem. Tech., Jan. 1973, pp. 47-52.
13. Castellano, J. A. and Brown, G. H., "Thermotropic Liquid Crystals: Part II. Current Uses and Future Ones," Chem. Tech., April 1973, pp. 229-235.
14. Castellano, J. A., "Now that the Heat Is Off, Liquid Crystals Can Show their Colors Everywhere," Electronics, v. 43, no. 14, July 1970, pp. 69-70.
15. Champa, R. A., "USAF Applications of Liquid Crystal Materials," AFML-TR-72-77, May 1972.
16. Fergason, J. L., Taylor, T. R., and Harsch, T. B., "Liquid Crystals and their Applications," Electro-Technology, v. 85, no. 1, Jan. 1970, pp. 41-50.
17. Kaye, D., "Liquid Crystals: Material with a Hot Future," Electronic Design, v. 19, Sept. 1970, pp. 76-81.
18. Cohen, S. E., "The Application of Liquid Crystals for Thermographic Testing of Bonded Structures," ASTIA AD 837835, 1967.
19. Davis, F., "Liquid Crystals: A New Tool for NDT," Research/Development, v. 18, no. 6, June 1967, pp. 24-27.
20. Dowden, W. A., "Cholesteric Liquid Crystals: A Review of Developments and Applications," Non-Destructive Testing, vol. 1, no. 2, Nov. 1967, pp. 99-102.
21. Woodmansee, W. E., "Aerospace Thermal Mapping Applications of Liquid Crystals," Applied Optics, v. 7, no. 9, Sept. 1968, pp. 1721-1729.
22. Perry, M. H., "Cholesteric Liquid Crystals and their Application to Space Technology," NASA General Working Paper, MSC-00152, Aug. 1969.

23. Crissey, J. T., Gordy, E., Fergason, J. L., and Lyman, R. B., "A New Technique for the Determination of Skin Temperature Patterns," Journal of Investigative Dermatology, v. 42, no. 2, Aug. 1964, p. 89.
24. Crissey, J. T., Fergason, J. L., and Bettenhausen, J. M., "Cutaneous Thermography with Liquid Crystals," Journal of Investigative Dermatology, v. 45, no. 5, Nov. 1965, p. 329.
25. Selawry, O. S., Selawry, O. H., and Holland, J. F., "The Use of Liquid Cholesteric Crystals for Thermographic Measurement of Skin Temperature in Man," Molecular Crystals, v. 1, no. 4, 1966, p. 495.
26. Cook, B. D. and Werchan, R. E., "Mapping Ultrasonic Fields with Cholesteric Liquid Crystals," Ultrasonics, April 1971, pp. 101-102.
27. Keilmann, F., "Infrared Interferometry with a CO₂ Laser Source and Liquid Crystal Detection," Applied Optics, v. 9, no. 6, June 1970, pp. 1319-1322.
28. Raad, T. and Meyer, J. E., "Nucleation Studies in Pool Boiling on Thin Plates Using Liquid Crystals," AICHE J., v. 5, 1971, pp. 1260-1261.
29. Ennulat, R. D. and Fergason, J. L., "Thermal Radiography Utilizing Liquid Crystals," Molecular Crystals and Liquid Crystals, v. 13, 1971, pp. 149-164.
30. Maple, R. D., "Utilization of Temperature Sensitive Liquid Crystals for Thermal Analysis and an Application to Transducer Investigations," Naval Underwater Systems Center TR 4235, 30 May 1972.
31. Cooper, T. E. and Groff, J. P., "Thermal Mapping, Via Liquid Crystals, of the Temperature Field Near a Heated Surgical Probe," J. Heat Transfer Trans. ASME, v. 95, no. 2, 1973, pp. 250-256.
32. Katz, R. G. and Cooper, T. E., "Liquid Crystal Display of the Temperature Fields Produced by Radio Frequency Emitting Electrodes," 26th ACEMB, Sept. 30 - Oct. 4, 1973, Conf. Proceed, p. 257.

33. Cooper, T. E. and Petrovic, W. K., "An Experimental Investigation of the Temperature Field Produced By a Cryosurgical Cannula," J. Heat Transfer, Trans. ASME, v. 96, no. 3, 1974, pp. 415-420.
34. Klein, E. J., "Application of Liquid Crystals to Boundary Layer Flow Visualization," AIAA 3rd Aerodynamic Testing Conference, AIAA paper 68-376, April 1968.
35. Klein, D. J., "Liquid Crystals in Aerodynamic Testing," Astronautics and Aeronautics, v. 6, no. 7, 1968, pp. 70-73.
36. Jones, R. A. and Hunt, J. L., "Use of Temperature-Sensitive Coatings for Obtaining Quantitative Aerodynamic Heat-Transfer Data," AIAA Journal, v. 2, no. 7, July 1964, pp. 1354-1356.
37. Jones, R. A. and Hunt, J. L., "An Improved Technique for Obtaining Quantitative Aerodynamic Heat-Transfer Data with Surface Coating Materials," Journal of Spacecraft and Rockets, v. 2, no. 4, July - August 1965, pp. 632-634.
38. Kaufman, L. G., Leng, J., and Johnson, A. R., "Exploratory Tests Using Temperature-Sensitive Paints to Obtain Hypersonic Heat Transfer Data on Spheres and on Fin-Plate Models," Grumman Research Dept. Memorandum RM-487, Sept. 1970.
39. Klein, E. J. and Margozzi, A. P., "Exploratory Investigation on the Measurement of Skin Friction by Means of Liquid Crystals," NASA TM X-1774, May 1969.
40. McElderry, E. D., "Boundary Layer Transition at Supersonic Speeds Measured by Liquid Crystals," Air Force Flight Dynamics Laboratory, FDMG Tm 70-3, June 1970.
41. Field, R. J., "Liquid Crystal Mapping of the Surface Temperature on a Heated Cylinder Placed in a Crossflow of Air," MS Thesis, Naval Post-graduate School, Monterey, Calif., March 1974.

42. Roshko, A., "Experiments on the Flow Past a Circular Cylinder at Very High Reynolds Numbers," J. of Fluid Mechanics, v. 10, May 1961, pp. 345-356.
43. Tani, I., "Low Speed Flows Involving Bubble Separations," in Progress in Aeronautical Sciences, v. 5, 1964, pp. 70-103.
44. Jones, G. W., Cincotta, J. J., and Walker, R. W., "Aerodynamic Forces on a Stationary and Oscillating Circular Cylinder at High Reynolds Numbers," NASA TR R-300, Feb. 1969.
45. Pope, A., Wind Tunnel Testing, 2nd ed., John Wiley and Sons, 1954, pp. 268-286.
46. Coder, D. W., "Location of Separation on a Circular Cylinder in Cross-flow As a Function of Reynolds Number," Naval Ship Research and Development Center Report 3647, Nov. 1971.
47. Giedt, W. H., "Investigation of Variation of Point Unit Heat-Transfer Coefficient Around a Cylinder Normal to an Air Stream," Trans. ASME, May 1949, pp. 375-381.
48. Kline, S. J. and McClintock, F. A., "Describing Uncertainties in Single-Sample Experiments," Mech. Engr., v. 75, Jan. 1953, pp. 3-8.
49. Auchenbach, E., "Influence of Surface Roughness on the Cross-flow Around a Circular Cylinder," J. Fluid Mechanics, v. 46, part 2, 1971, pp. 321-335.
50. Fergason, J. L., "Liquid Crystals in Nondestructive Testing," Applied Optics, v. 7, no. 9, Sept. 1968, pp. 1729-1737.
51. Parker, R., "Transient Surface Temperature Response of Liquid Crystal Films," Lawrence Livermore Laboratory, Rept. UCRL-73583, Dec. 1971.

INITIAL DISTRIBUTION LIST

No. Copies

| | | |
|----|--|---|
| 1. | Commander Naval Weapons Center China Lake, California 93555 Attn: | |
| | Mr. T. Inouye (Code 4533) | 5 |
| | Mr. C. Maples (Code 453) | 1 |
| | Mr. C. F. Markarian (Code 4061) | 2 |
| | Mr. H. C. Schafer (Code 45330) | 1 |
| | Dr. R. Ulrich (Code 4570) | 1 |
| 2. | Library Naval Postgraduate School Monterey, California 93940 | 2 |
| 3. | Dean of Research Naval Postgraduate School Monterey, California 93940 | 1 |
| 4. | Director Defense Documentation Center 5010 Duke Street Alexandria, Virginia 22314 | 2 |
| 5. | Department of Mechanical Engineering, Code 59 Naval Postgraduate School Monterey, California 93940 | 1 |
| 6. | Professor Thomas E. Cooper, Code 59Cg Naval Postgraduate School Monterey, California 93940 | 5 |
| 7. | LCDR John F. Meyer, Code 59 Naval Postgraduate School Monterey, California 93940 | 5 |
| 8. | Lt. Richard J. Field, Code 59 Naval Postgraduate School Monterey, California 93940 | 5 |
| 9. | Chief of Naval Research Arlington, Virginia 22217 | 1 |

U164540

DUDLEY KNOX LIBRARY - RESEARCH REPORTS



5 6853 01070289 7